Summer 2016

Yeast Dynamin Functions With ESCRT-II At The Late Endosome And Potential Roles With Novel Binding Partners

Bryan Thien Banh

YEAST DYNAMIN FUNCTIONS WITH ESCRT-II AT THE LATE ENDOSOME AND POTENTIAL ROLES WITH NOVEL BINDING PARTNERS

A Masters Thesis

Presented to

The Graduate College of

Missouri State University

In Partial Fulfillment

Of the Requirements for the Degree

Master of Science, Biology

By

Bryan T Banh

July 2016

YEAST DYNAMIN FUNCTIONS WITH ESCRT-II AT THE LATE ENDOSOME AND POTENTIAL ROLES WITH NOVEL BINDING PARTNERS

Biology

Missouri State University, July 2016

Master of Science

Bryan T Banh

ABSTRACT

Yeast dynamin, Vps1, is a dynamic protein implicated in multiple trafficking pathways and at several cellular locations including the Golgi, endosome, and vacuole. Previous studies have found that Vps1 genetically and physically interacts with several ESCRT-II (Vps22, Vps36) and ESCRT-III (Vps2, Vps24) components. In light of these findings, little is known about how Vps1 functions with the ESCRT system. In my study, I have mapped the interaction domains between Vps1 and Vps22/Vps36 as well as explored the potential roles of these proteins during the targeting of vacuolar hydrolase, Cps1. My results support the idea of Vps1 working at the endosomal membrane and interacting with ESCRT-II towards the N-terminal end of its Vps22/Vp36 lobe. Additionally, a yeast two-hybrid library screen was performed in search of Vps1 binding partners. Here, I present seventeen novel binding partners. Based on these results, I have proposed a potential role for Vps1 in regulating chitin synthases during yeast cellular budding.

KEYWORDS: Vps1, ESCRT, Protein Sorting, MVB, Yeast-Two Hybrid Screen

This abstract is approved as to form and content

_____

Dr. Kyoungtae Kim
Chairperson, Advisory Committee
Missouri State University

YEAST DYNAMIN FUNCTIONS WITH ESCRT-II AT THE LATE ENDOSOME

AND POTENTIAL ROLES WITH NOVEL BINDING PARTNERS

By

Bryan T Banh

A Masters Thesis
Submitted to the Graduate College
Of Missouri State University
In Partial Fulfillment of the Requirements
For the Degree of Master of Science, Biology

July 2016

Approved:

_____
Dr. Kyoungtae Kim

_____
Dr. Laszlo Kovacs

_____
Dr. Ryan Udan

_____
Dr. Julie Masterson, Dean, Graduate College

ACKNOWLEDGEMENTS

I wish to express my deepest thanks to Dr. Kyoungtae Kim for all that he has done these past few years that have aided in my academic and professional development. I would also like to give Dr. Laszlo Kovacs and Dr. Ryan Udan a very big thank you for dedicating their time and knowledge as my thesis committee members and as my professors. Additionally, I would like to acknowledge my colleagues Shiva Kumar Goud Gadila, Uma Saimani, Pelin Makaraci, Sara Woodman, Hyoeun McDermott, Christopher Trousdale, John Short, Mariel Delgado Cruz, and Ashley Smock for their assistance in my research. Next, I would like to thank the Biology Department and the Graduate College for their financial support. Finally, I would like to thank my friends and family for their support and encouragement.

TABLE OF CONTENTS

Introduction....1
- Early Endosomal Regulatory Elements....2
- Early Endosome to Late Endosome Maturation....4
- Cargo Sorting in Multivesicular Bodies....5
- Dynamin and Its Role in Membrane Sorting....8

Hypothesis and Goals....11

Materials and Methods....13
- Strains/Cell Maintenance....13
- Plasmid Construction....13
- One-on-One Yeast Two-Hybrid Assay....14
- Fluorescent Microscopy....15
- Construction of Bait Vector and Yeast cDNA Library....15
- Yeast Two-Hybrid Screen....16
- Genomic Analysis....17

Results....22
- Vps1 Physically Interacts with ESCRT-II Subunits....22
- Vps1 and ESCRT-II Subunits Colocalize at the Endosome....22
- Loss of Vps1 or Inactivation of the GTPase Activity of Vps1 Resulted in Cps1 Mistargeting....23
- Yeast-Two Hybrid Library Screen for Vps1 Binding Partners....25

Discussion....27

References....43

LIST OF TABLES

Table 1. Yeast Strains Used in This Study. 18

Table 2. Bacterial Plasmids Used in This Study.....21

Table 3. Vps1 Yeast Two-Hybrid Screen.....41

LIST OF FIGURES

Figure 1. Endosome Maturation 32

Figure 2. Intralumenal Vesicle formation by ESCRT 33

Figure 3. Localization of Vps1 in *S. cerevisiae*. 34

Figure 4. Mapping of Domains of Vps22 and Vps36 Required for Vps1 Binding 35

Figure 5. Vps1 and ESCRT-II Subunits Localize to the Endosome.....36

Figure 6. mRFP-Cps1 is Mistargeted in Vps1 and ESCRT-II and –III Mutant Cells 37

Figure 7. Yeast Two-Hybrid Genome-Wide Screen for Searching Vps1 Binding Partners in *S. cerevisiae* 38

Figure 8. A Potential Model of Vps1 and ESCRT-II Interaction at the Endosome. 39

Figure 9. Interaction Mapping of Vps1 in Chitin Deposition.....40

INTRODUCTION

Eukaryotic cells maintain homeostasis through synthesis, transport, and degradation of important proteins. Our current understanding classifies protein traffic into several major pathways. Anterograde trafficking is typically referred to as the delivery of cargo proteins from the rough ER to the Golgi where they can be sorted for the lysosome (vacuole) or the plasma membrane (Wang and Wu, 2012). In contrast, retrograde transport is typically associated with the reverse traffic for retrieval or recycling of diverse cargoes, from endosomal compartments to the Golgi or to the plasma membrane (Chia et al., 2013). In addition, endocytosis and exocytosis/secretion pathways involve movement of materials into or out of the cell, respectively (Elkin et al., 2016; Thorn et al., 2016). Finally, nutrients and misfolded proteins transported to the lysosome through the endosomal system are referred to as the degradation pathway (Lilienbaum, 2013). This introduction will primarily focus on the degradation traffic of ubiquitinated cargo from the early endosome (EE) to the lysosome via late endosome (LE) maturation.

Defects of key regulators in the degradation trafficking have been strongly linked to neurodegenerative diseases (Kim et al., 2016; Liu et al., 2011; Munsie et al., 2015), muscular diseases (Lin et al., 2016; Neel et al., 2015), and tumorigenesis (Chen et al., 2016; Silva et al., 2016). For example, defects in myotubularin, a protein involved in regulating the dynamics of endosomal maturation by dephosphorylating phosphatidylinositol 3-phosphate (PI3P) and phosphatidylinositol 3,5-bisphosphate (PI3,5P)**,** have been linked to myotubular myopathy (Goddard et al., 2015). While the precise pathological mechanism is still unknown, defective myotubularin activity in

membrane regulation likely delays or diminishes endosomal maturation (Lawlor et al., 2016). Certain pathogens can also take advantage of machinery in the degradation pathway. Human Immunodeficiency Virus-1 (HIV-1) affects the degradation pathway by intervening with the endosomal sorting complex required for transport (ESCRT) system. HIV-1 hijacks ESCRT machinery during the late stages of its replication cycle to aid in membrane budding that lead to viral exit (Meng et al., 2015). Mammalian and yeast systems possess many functionally conserved pathways. This has allowed the application of major discoveries in yeast to their mammalian counterparts. Due to this fact, I will be referring to some of the proteins by both yeast and mammalian aliases or by the system which is best understood.

Early Endosomal Regulatory Elements

The EE is an important organelle involved in sorting and targeting of cargo. On the endosomal membrane, Rab and Arf GTPases act as key regulators by controlling cargo sorting and recruiting (Donaldson and Jackson, 2011; Dutta and Donaldson, 2015; Stenmark, 2009). Vps21/Rab5 (Yeast/Mammalian) is recognized as a major factor for EE regulation due to its role in recruitment of effectors and endosome-to-endosome fusion (Huotari and Helenius, 2011; Zeigerer et al., 2012). Similar to other Rab-GTPases, Rab5 activity is mainly controlled through activation by guanine exchange factors (GEFs) (Blumer et al., 2013). Rab5's main GEF is Rabex-5 which is recruited to the EE in complex with Rabaptin5 (Rbpt5) (Blumer et al., 2013; Lippe et al., 2001). While Rbpt5 physically interacts with Rab5, it is not required for Rab5 activation, suggesting that it is

primarily involved in Rabex-5 recruitment (Delprato and Lambright, 2007; Zhu et al., 2010).

Additionally, phospholipids serve as an identity marker for membranes of various organelles to help recruit cytoplasmic factors based on their lipid binding abilities. At the EE, active Rab5 activates phosphoinositide 3-kinase (PI3K), or Vps34 in yeast, to synthesize PI3P (Bissig and Gruenberg, 2013). A positive feedback loop occurs when increased of PI3P increases Rab5 and Rabex5 recruitment to the EE and further activating Vps34 (Poteryaev et al., 2010). The prevalence of PI3P on the EE allows recruitment of specific proteins containing lipid binding domains such as C2, FYVE, PX, PH, GRAM, and GLUE (Marat and Haucke, 2016). Among these proteins, Rab5 effectors, early endosome antigen 1 (EEA1) and Rabenosyn-5, are recruited to the EE, which become important factors during endosomal fusion (Bissig and Gruenberg, 2013; Marat and Haucke, 2016; Nielsen et al., 2000).

Sorting at the EE can occur in several ways. Certain cargo possess specific membrane-bound receptors that help facilitate their transport. Vps10p is a classical example of a cargo receptor, which associates with carboxypeptidase Y (CPY) and cycles between the Golgi and the endosomal system (Cooper and Stevens, 1996). Vps10p possesses a luminal domain capable of interacting with CPY and a cytosolic tail that allows targeting of Vps10p (Dennes et al., 2002). At the Golgi and EE, CPY remains bound to Vps10p, but disassociates under the acidic condition of the LE (Bonifacino and Rojas, 2006). Another method of targeting to the lysosome is through ubiquitination . Ubiquitinated cargo are sorted by the ESCRT system through ubiquitin-mediated interaction. One example of this is carboxypeptidase S 1 (Cps1). Cps1 is a vacuolar

hydrolase that becomes ubiquitinated at the Golgi and is sequestered into intralumenal vesicles (ILVs) by ESCRT at the EE as later described (Shields et al., 2009). Furthermore, misfolded proteins coming from the plasma membrane can be targeted for degradation in a similar pathway as mentioned above. For example, Ste2 is a yeast pheromone receptor that is internalized upon ubiquitination at its cytosolic tail (Shenoy, 2007). Once internalized, it is deubiquitinated, sorted into ILVs, and targeted for the vacuole (Urbe, 2005).

Early Endosome to Late Endosome Maturation

EE traveling towards the lysosome undergoes a series of changes that help organize cargo into ILVs as well as alters the endosome's overall morphology (Figure 1). Endosomal maturation allows recruitment of a new set of proteins associated with LE function and leading to lysosomal fusion. One major change that occurs when the Rab5-dominant endosome transitions into a Rab7-dominant endosome termed the Rab switch. This process is assisted by Mon-1/Sand-1, which displaces Rabex5, thus halting the positive feedback loop as described above (Poteryaev et al., 2010). Sand-1 and Czz1 then recruit and activate Rab7 (Poteryaev et al., 2010; Yasuda et al., 2016).

In addition to the Rab switch, another significant change occurs when the PI3P-enriched membrane transitions into a PI3,5P_2-dominant membrane. Reduction of PI3P can be attributed to the dephosphorylation by myotubularins (Robinson and Dixon, 2006) or the phosphorylation and conversion of PI3P to PI3,5P_2 by Fab1/PIKfyve (Zolov et al., 2012). Furthermore, PI3P levels can be controlled by other factors such as SORF-

1/WDR91 and SORF-2/WDR81, which work in complex with BEC-1/Beclin1 to negatively regulate PI3K activity (Liu et al., 2016).

Cargo Sorting in Multivesicular Bodies

Another major characteristic of endosomal maturation is the formation of ILVs in the endosome, and the endosome that carries ILVs is referred to as multivesicular bodies (MVBs) or late endosomes. The cargo sorting into ILVs within the endosome is assisted by the ESCRT system (Henne et al., 2011). The ESCRT system is composed of ESCRT-0, ESCRT-I, ESCRT-II, and ESCRT-III and the disassembly complex Vps4-Vta1, which facilitates the release of ESCRT-III upon formation of the ILV. As the endosome matures, more ILVs accumulate in the lumen of the LE. Cargos sorted into ILVs are then released into the lumen of the lysosome upon LE-lysosome fusion.

The ESCRT system operates through a series of sequential recruitment of protein complexes based on their intrinsic lipid and cargo binding abilities, as well as interactions between ESCRT complexes (Figure 2). ESCRT-0, comprised of Vps27/HRS and Hse1/STAM1, initiates ubiquitinated cargo sorting when recruited to the EE (Ren and Hurley, 2010). ESCRT-0 possesses the highest affinity to PI3P among all other ESCRT complexes through its Vps27 FYVE domain (Raiborg et al., 2001) and interacts with ubiquitinated cargo through its VHS domain and a ubiquitin interacting motif (UIM) that exist on both Hse1 and Vps27 (Ren and Hurley, 2010; Takahashi et al., 2015). ESCRT-0's ability to sort cargo may also be attributed to its interaction with other ubiquitin binding proteins such as USP8 and UBE4B (MacDonald et al., 2014; Sirisaengtaksin et al., 2014). Ultimately, ESCRT-0 helps localize other ESCRT complexes to the cluster of

ubiquitinated cargo, which promotes the formation of the invaginated pit at the ubiquitinated cargo cluster (Wollert and Hurley, 2010).

ESCRT–I, consisting of Vps23/TSG101, Vps28, Vps37/Vps37A-D, and Mvb12/MVB12a, is the next complex to be recruited (Boura et al., 2011; Kostelansky et al., 2007). Interaction between Vps27/HRS (ESCRT-0) and Vps23/TSG101 (ESCRT-I), as well as the lipid binding domain on Vps37, aids in ESCRT-I localization (Kostelansky et al., 2006). Once recruited, ESCRT-I helps sort ubiquitinated cargo through its ubiquitin E2 variant (UEV) domain on Vps23 (Teo et al., 2004b). ESCRT-II, comprising of Vps22/Eap30, Vps36/Eap45, and two Vps25/Eap20, is then recruited to the endosome through Vps28 (ESCRT-I) and Vps36 (ESCRT-II) interaction (Gill et al., 2007; Wollert and Hurley, 2010) and by its interaction with PI3P using Vps36's N-terminal GLUE domain as well as a predictive domain on Vps22 (Im and Hurley, 2008). Similar to the previous ESCRT complexes, ESCRT-II is also capable of interacting with ubiquitin through Vps36's GLUE domain (Gill et al., 2007; Shields et al., 2009). Under *in vitro* conditions, ESCRT-I and –II complexes in combination were shown to be sufficient in forming small inward buds in giant unilamellar vesicles without ESCRT-0 (Wollert and Hurley, 2010). However, studies demonstrated that ESCRT-I alone is not essential in ILV formation other than to recruit ESCRT-II for the activation of ESCRT-III (Babst et al., 2002; Mageswaran et al., 2015).

Invaginated ILVs carry ubiquitinated cargo, but the direct mechanism of cargo loading into the ILV is poorly understood. In one proposed model, ubiquitinated cargo is handed off from one complex to another in a conveyor belt-like process (Hurley and Emr, 2006). This model suggests that the interaction between the ESCRT complexes helps

mediate the exchange of ubiquitinated cargo based on the order of their recruitment. It predicts that ESCRT-III is located closer to the forming ILV, while ESCRT-0 is farther away. In this scenario, the ubiquitinated cargoes are handed off down the line from ESCRT-0 to ESCRT-III. However, when ESCRT-II was knocked down, the rate of degradation for plasma membrane protein epidermal growth factor was not affected, suggesting that ESCRT-II was not essential for certain ubiquinated cargo (Bowers et al., 2006). Another model proposes that ubiquitinated cargo is clustered at the site of invagination before ILV formation. Currently, this is the leading model in cargo sorting, as recent studies provide more evidence to support this hypothesis. In this scenario, ESCRT-0 initiates localization of the cargo and recruits the sequential ESCRT components around the cluster (Nickerson et al., 2007). As the ILV pit is formed, the earlier ESCRT components are released and the cargo is deubiquitinated (Henne et al., 2011).

Once the ILV is ready for fission, ESCRT-III, consisting of Vps2/Chmp2A-B, Vps20/Chmp6, Snf7/Chmp4A-C, and Vps24/Chmp3, is recruited to the invaginated pit. These components remain inactive in the cytoplasm until they are recruited to the endosome. Traditionally, it was conceived that ESCRT-I/II triggers the activation of Vps20 (ESCRT-III) leading to Snf7 polymerization around the neck of the invaginating pit (Henne et al., 2011; Teis et al., 2010). However, a recent study revealed that ESCRT-0 and Bro1 may work in a parallel pathway to activate Snf7 independent of ESCRT-I/-II (Tang et al., 2016). At the cytoplasmic end of the polymerized Snf7 filament, Vps24 caps off the structure and recruits Vps2. While the other three components of ESCRT-III appear to be vital for ILV fission, Vps2 does not appear to play an essential role in this

process, but is likely involved in recruiting the disassembly complex Vps4 (Wollert et al., 2009). The assembled Snf7 filament forms a spiral around the neck of the invaginated pit that further tubulates the membrane leading to fission of the ILV (Chiaruttini et al., 2015). While Vps4 was mainly implicated in ESCRT-III disassembly, it is notable to mention that Vps4 appears to also play a role in ILV fission as well (Nickerson et al., 2010). It's hypothesized that Vps4 binds to ESCRT-III through its C-terminal MIM motif and releases the tension during disassembly process leading to fission of the ILV (Henne et al., 2013).

Dynamin and Its Role in Membrane Sorting

Among the diverse array of proteins involved in cellular trafficking, my focus will be on yeast dynamin, Vps1. Dynamin is a membrane remodeling GTPase, best characterized by its role in endocytic fission and vesicle fusion (Anantharam et al., 2011; Kulkarni et al., 2014b; Sundborger and Hinshaw, 2014). Mammalian systems possess three isoforms of dynamin proteins; dynamin1, 2, and 3, sharing 80% homology between one another. Dynamin-1 and dynamin-3 are primarily found in nerve cells, while dynamin-2 is expressed ubiquitously (Cao et al., 1998).

Classical dynamins are composed of five major domains, with an N-terminal GTPase (G-domain), a middle domain (stalk), a pleckstrin homology domain (PH), a GTPase effector domain (GED), and a C-terminal proline-rich domain (PRD) (Chappie and Dyda, 2013). In addition, a small bundle signal element (BSE) region exists on both sides of the G-domain as well as the C-terminal end of the GED, and BSE is required for bringing the G-domain and stalk/GED together in dynamin's tertiary structure (Chappie

and Dyda, 2013). During endocytosis, dynamin self-assembles through their stalk-to-stalk interactions in a criss-cross manner (Faelber et al., 2012). As a result, two GTPase heads are orientated on the same side, while the lipid binding PH domains are situated on the opposite side of the catalytic GTPase heads (Chappie and Dyda, 2013). A tetrameric dynamin forms in the cytoplasm as two dimers joined by a short stretch located at the stalk-GED region (Chappie and Dyda, 2013). Dynamin tetramers are then recruited to the membrane via their PH and PRD domains, followed by a high-order assembly around the neck of the invaginated pit (Faelber et al., 2012; Mehrotra et al., 2014). A conformational change in the BSE region driven by the association and hydrolysis of GTP allows the homo-oligomeric structure to constrict and elongate, which results in fission of the nascent vesicle (Chappie et al., 2011; Faelber et al., 2012).

The budding yeast, Saccharomyces cerevisiae, expresses three dynamin-like proteins (DLPs) homologous to mammalian dynamins. Dynamin-related GTPase (Dnm1) and mitochondrial genome maintenance (Mgm1) primarily function in fission and fusion at the mitochondrial membrane (Abutbul-Ionita et al., 2012; Mears et al., 2011), whereas vacuolar sorting protein (Vps1) localizes at a wider range of cellular structures, including the Golgi, endosome, vacuole, peroxisome and plasma membrane (Figure 3) (Alpadi et al., 2013; Hayden et al., 2013; Kuravi et al., 2006; Nothwehr et al., 1995; Smaczynska-de et al., 2015; Williams and Kim, 2014). Among its diverse roles, Vps1 was initially characterized in cargo sorting at the late Golgi due to the fact that vps1 mutant cells exhibited an impaired carboxypeptidase Y (CPY) trafficking bound for the vacuole, namely in anterograde traffic (Nothwehr et al., 1995; Robinson et al., 1988). Severe defects in the retrograde traffic from the endosome to the late Golgi have also been

observed in Vps1-deficient cells (Arlt et al., 2015; Chi et al., 2014; Lukehart et al., 2013). Additionally, endocytosis and degradation traffic from the endosome to the vacuole was disrupted in *vps1* mutant strains (Hayden et al., 2013; Smaczynska-de et al., 2015). Together, this evidence suggests Vps1's implication in a broad spectrum of membrane traffic pathways.

In addition, evidence has supported Vps1's role in membrane remodeling required for membrane fusion and fission. Upon oligomerization, Vps1 can interact with and tubulate liposomal membranes *in vitro* (Smaczynska-de Rooij et al., 2010). Vps1-mediated scission of the nascent vesicle during endocytosis appears to depend on the negatively-charged glutamate residue at position 461 and phosphorylation of the 599 residue (Palmer et al., 2015; Smaczynska-de et al., 2015). Surprisingly, Vps1 also plays a role in vacuolar homotypic fusion (Alpadi et al., 2013), which requires Vps1's self-assembly ability (Kulkarni et al., 2014b).

Significant progress has been made in the past two decades for understanding the molecular features of dynamin-related protein functioning in a variety of cellular processes. However, many details regarding the precise action mode of Vps1 in these traffic pathways and its binding partners at different sub-cellular locations still elude us. An investigation of its interactions with different partners may provide deeper insights into potential or uncharacterized roles of Vps1.

HYPOTHESIS AND GOALS

My study aims to understand Vps1's role in the Golgi-to-vacuole pathway as well as its broader implications through a library screen. As previously mentioned, Vps1 is a membrane remodeling protein that localizes to the Golgi, endosome, and vacuole (Alpadi et al., 2013; Hayden et al., 2013; Kulkarni et al., 2014b). The clue for the mechanism of Vps1's localization to the endosome came from the finding that it interacts directly with PI3P, a phospholipid enriched in endosomal membrane (Smaczynska-de et al., 2015). Interestingly, it was found that Vps1 plays a role in the formation of ILV in the lumen of early endosomes due to the fact that loss of Vps1 causes cells to have fewer and larger ILVs (Chi et al., 2014). Furthermore, our lab has previously determined that Vps1 genetically interacts with Vps22, 23, 24, 25, 28, 26 and 37 (Hayden et al. 2013) and physically interacting with Vps2, 22, 36, and 24 in yeast two-hybrid assay (Thesis of Hyoeun McDermott and Chris Trousdale). Both ESCRT and Vps1 have been well characterized in membrane remodeling and protein sorting. However, many aspects in the molecular mechanism of how they function is still unknown. Here, my project aims to understand the underlying mechanism of Vps1 and ESCRT's significance in targeting of cargo towards the vacuole. The study focuses on the following topics.

1) Mapping Vps1 and ESCRT-II domain interaction. Based on the crystal structure of ESCRT-II, I hypothesized that Vps1 would interact at the exposed N-terminal domain of ESCRT-II's Vps22/36 lobe. To test this, I performed a yeast two-hybrid interaction assay with truncations of Vps1 and Vps22/36 fragments.
2) Vps1 and ESCRT-II localizes to the endosome. Previous work has shown localization of these proteins to the endosome, however, colocalization has not been observed. I hypothesize that Vps1 and ESCRT-II subunits Vps22 and Vps36 would colocalize at the endosome. This hypothesis was tested.
3) Vps1 and ESCRT subunits are involved in ubiquitinated cargo targeting to the vacuole. I hypothesize that upon knockout of Vps1 or ESCRT-II and –III

subunits, Cps1, a vacuolar hydrolase, would be mistargeted. To test this, Cps1 was tagged with a red fluorescent protein and expressed in yeast cells that are either deficient or have a mutant version of Vps1 or a ESCRT subunit.
4) Library screen of Vps1 may reveal novel roles. I will be reporting the remaining novel Vps1 binding partners based from Hyoeun McDermott's thesis as well as perform a validation assay. Here, I will connect the data acquired from my yeast two-hybrid library screen to propose a new role for Vps1.

Taken together, I propose that yeast dynamin Vps1 works in parallel or synergistically with the ESCRT system in cargo sorting and formation of ILVs during endosomal maturation. Additionally, partners from the library screen may implicate Vps1 in novel roles.

MATERIALS AND METHODS

Strains/Cell Maintenance

Saccharomyces cerevisiae Y187, Y2HGOLD and *Escherichia coli* HST08, acquired through Clontech, *S. cerevisiae* BY4741 from Invitrogen and KKY248, KKY249, KKY250, KKY251, and KKY252 were acquired from Dr. Cai's lab (University of Singapore) (Table 1). All cells were stored at -80˚C until use. Plasmid vectors pGADT7-Rec (prey) and pGBKT7 (bait) were used as an overexpression vector for the protein of interest tagged with the Activator Domain (in prey) or Binding Domain (in bait), respectively (Table 2). Stellar competent *E. coli* cells carrying these vectors were kept at -80˚C and purified vectors were kept at -20˚C until use. During cell culturing, yeast cells were grown in 30˚C and bacterial cells at 37˚C.

Plasmid Construction

Purified genomic DNA from *S. cerevisiae* (BY4741, Invitrogen) was used as a template for the amplification of target DNA sequences using Phusion Green High-Fidelity DNA Polymerase (Thermo Scientific), prior to molecular cloning processes. For my yeast two-hybrid assay, In-Fusion HD cloning kit (Clontech) was used to insert a gene of interest into a target vector. The PCR-amplified DNA sequences of Vps1 full-length and 3 individual domains of Vps1 (GTPase, Middle, and GED) were inserted into EcoRI and BamHI sites of the bait vector (pGBKT7). The PCR-amplified DNA sequences of Vps22 (1-100aa), Vps22 (80-233), Vps36 (1-236aa), and Vps36 (236-566aa) were ligated into the prey vector pGADT7 using EcoRI and BamHI sites. Spa2

(2476-4401 bp) and Ste24 (1195-1362 bp) sequences were ligated into pGADT7 vector using XmaI and BamHI restriction sites.

The TEF promoter sequence was PCR-amplified from pOK489 (Obara et al., 2013) and inserted into *S. cerevisiae* shuttle vectors, pRS314 and pRS315, between the SacI and NotI restriction sites. GFP-Vps1 was constructed on both pRS314 and pRS315 vectors. Briefly, the GFP sequence was ligated into BcuI and PstI sites, and the Vps1 sequence was cloned between the PstI and SalI sites. Vps22-and Vps36-mRFP vectors were constructed on pRS314 using BcuI and PstI sites for Vps22 or Vps36 and SalI and KpnI sites for mRFP. The ligated vectors were then transformed into Stellar competent *E. coli* cells (Clontech). The identity of the inserts was confirmed by bacterial colony PCR and restriction digestion. mRFP-Cps1 was generously donated by Dr. Kihara (Obara et al., 2013) and GFP-Pep12 was donated by Dr. Fujimura-Kamada (Furuta et al., 2007).

One-on-One Yeast Two-Hybrid Assay

Yeast mating was performed according to Matchmaker® Gold Yeast Two-Hybrid System (Clontech). The prey vector (pGADT7) harboring a gene that codes for a tentative binding partner of Vps1 was transformed into Y187 haploid yeast (KKY 1255), while the bait (pGBKT7) vector with Vps1 or its fragmental sequences was transformed into Y2HGOLD haploid yeast (KKY1254) by a yeast transformation protocol previously described (Chen et al., 1992). The haploid cells were mated at 30˚C overnight in a single flask of 2xYPDA. The mated cells were then plated on Double Drop Out (DDO; -Leu, -Trp) medium and replicated onto Triple Drop Out (TDO; -Leu, -Trp, -His) and Quadruple Drop Out (QDO; -Leu, -Trp, -His, -Ade) plates.

Fluorescent Microscopy

Confocal microscopy analysis of GFP- or mRFP-fused proteins was performed using an Olympus IX81-ZDC inverted fluorescence microscope equipped with a Spinning-Disc confocal system (Yokogawa CSU-X1M1L) and Slidebook v6. The yeast strains expressing the fusion proteins were grown to log phase (0.6-0.8 OD), and fluorescence images were taken by an Electron Amplified CCD (ImagEM, Hammamatsu) with 100 ms exposure time.

Construction of Bait Vector and Yeast cDNA Library

Purified genomic DNA from *S. cerevisiae* (BY4741, Invitrogen) was used as a template for amplification of *VPS1* DNA sequence using Phusion Green High-Fidelity DNA Polymerase (F-534L, Thermo Scientific) with forward primer 5'CATGGAGGCCGAATTCATGGATGAGCATTTATTTTCTAC 3' and reverse primer 5'GCAGGTCGACGGATCCAACAGAGGAGACGATTTGACTAG 3'. The amplified sequence was ligated by using In-Fusion® HD Cloning Kit (Clontech) into the linearized BD (DNA Binding Domain, pGBKT7) vector using EcoRI and BamHI. The recombinant vector was then transformed into Stellar Competent *E. coli*, using the corresponding protocol PT5055-2 from Clontech. The cells were plated on LB agar plates, containing 25 µg/ml kanamycin. Positive colonies were confirmed by bacterial colony PCR and restriction enzyme digestion with EcoRI and BamHI. The bait vector, pGBKT7-Vps1, was then purified using PureYieldTM Plasmid Miniprep System (A1223, Promega), prior to performing a one-step transformation into competent Y2HGOLD yeast cells as previously described (Chen et al., 1992).

A library of potential Vps1 binding partners was constructed in AD (Activation Domain, pGADT7-rec) vector using Clontech's Make Your Own "Mate & Plate™" Library System (PT4085-1). Total mRNA was first extracted from wild type *S. cerevisiae* (KKY002) using Masterpure Yeast RNA Purification Kit (MPY03100, Epicentre). The purified mRNA product was then converted into cDNA using SMART MMLV Reverse Transcriptase with CDS III primers poly-A specific primers containing EcoRI and BamHI restriction sites. The cDNA product was amplified using Long Distance PCR and purified with CHROMA SPIN+TE-400 Columns. Following Matchmaker Yeast Transformation System 2 Usual Manual (Clontech), 5 µg of the purified cDNA and 3 µg pGADT7-Rec (Clontech) were co-transformed into Y187 strain, allowing *in vivo* recombination in yeast. Transformants were plated on selective media, lacking leucine (SD/-Leu), and were incubated at 30°C for 3-4 days.

Yeast Two-Hybrid Screen

The yeast two-hybrid screen was performed using the Matchmaker Gold Yeast Two-Hybrid System (Clontech) with minor adjustments. The harvested prey library pool (pGADT7-Rec cDNA) was mated with the bait strain (pGBKT7-Vps1) according to Clontech's Mate and Plate System. The culture was then plated on Triple Drop Out (-leu, -trp, -his), Quadruple Drop Out (-leu, -trp, -his, -ade), and Double Drop Out with X-alpha-gal and Aureobasidin (DDO/X/A) plates for 3-5 days for screening. Colonies that survived on the QDO and turned blue on DDO/X/A were selected for DNA sequencing. The vectors were then isolated from the positive colonies using Zymoprep™ Yeast Plasmid Miniprep I (D2001, Epigenetics Company). These vectors were amplified in

Stellar competent *E. coli* cells as previously described and grown in LB medium containing ampicillin. The vectors were then isolated from *E. coli* using QIAGEN Miniprep Kit and then quantified using an Implen Nanophotometer.

Genomic Analysis

Vectors containing the gene of interest were isolated from positive colonies and delivered to a biotechnology company (Eurofins) for sequencing. Proteins were identified by comparing genetic data using Basic Local Alignment Search Tool (BLAST) search from the National Center for Biotechnology Information (NCBI) and Saccharomyces Genomic Database (SGD) websites.

Table 1. Yeast Strains Used in My Study

Strain Number	Source	Genotype
KKY 0002	Invitrogen	MAT a *his3Δ1 leu2Δ0 met15Δ0 ura3Δ0*
KKY 0248	(Yu and Cai, 2004)	MAT a *ade2-1 trp1-1 can1-100 ura3-52 leu2-3,112 vps1Δ::LEU2 his3-11,15::HIS3*
KKY 0249	(Yu and Cai, 2004)	KKY 248 *15::HIS3-Vps1-3myc*
KKY 0250	(Yu and Cai, 2004)	KKY 248 *15::HIS3-vps1^{K42E}-3myc*
KKY 0251	(Yu and Cai, 2004)	KKY 248 *15::HIS3-vps1^{S43N}-3myc*
KKY 0252	(Yu and Cai, 2004)	KKY 248 *15::HIS3-vps1^{G315D}-3myc*
KKY 0270	(Nannapaneni et al., 2010)	MAT a *his3Δ leu2Δ met15Δ ura3Δ Vps1-C-term domain::HIS*
KKY 0343	This study	MAT α *his3Δ uraΔ leuΔ trpΔ lysΔ*
KKY 0352	This study	KKY 343 *vps1Δ::KanMx6*
KKY 0866	Invitrogen	MAT a *hisΔ leuΔ uraΔ metΔ vps36Δ::KanMx6*
KKY 1034	This study	KKY 002 *vps22Δ::HIS*
KKY 1061	This study	KKY 002 *vps2Δ::HIS*
KKY 1062	This study	KKY 002 *vps24Δ::HIS*
KKY 1254	Clontech	MAT a *trp1-901 leu2-3 112 ura3-52 his3-200 gal4Δ gal80Δ LYS2::GAL1$_{UAS}$–Gal1$_{TATA}$–His3 GAL2$_{UAS}$–Gal2$_{TATA}$–Ade2 URA3::MEL1$_{UAS}$–Mel1$_{TATAA}$ UR1-C MEL1*
KKY 1255	Clontech	MAT α *ura3-52 his3-200 ade2-101 trp1-901 leu2-3 112 gal4Δ gal80Δ met URA3::GAL1$_{UAS}$–Gal1$_{TATA}$–LacZ MEL1*
KKY 1272	Clontech	KKY 1254 *pGBKT7-Lamin*
KKY 1273	Clontech	KKY 1255 *pGADT7-SV40 large T antigen*
KKY 1274	Clontech	KKY 1254 *pGBKT7-p53*
KKY 1275	This study	KKY 1254 *pGBKT7-Vps1*
KKY 1304	This study	KKY 1273 x KKY 1274
KKY 1305	This study	KKY 1272 x KKY 1274
KKY 1358	This study	KKY 1255 *pGADT7-Vps22*
KKY 1359	This study	KKY 1255 *pGADT7-Vps25*
KKY 1360	This study	KKY 1255 *pGADT7-Vps28*
KKY 1369	This study	KKY 1275 x KKY 1358
KKY 1370	This study	KKY 1275 x KKY 1378
KKY 1371	This study	KKY 1275 x KKY 1359
KKY 1372	This study	KKY 1275 x KKY 1360
KKY 1373	This study	KKY 1275 x KKY 1379
KKY 1374	This study	KKY 1255 *pGADT7-Vps36*
KKY 1378	This study	KKY 1255 *pGADT7-Vps24*
KKY 1379	This study	KKY 1255 *pGADT7-Vps37*
KKY 1390	This study	KKY 1275 x KKY 1374
KKY 1438	This study	KKY 1254 *pGBKT7-Vps1 GTPase*
KKY 1439	This study	KKY 1254 *pGBKT7-Vps1 Middle*
KKY 1440	This study	KKY 1254 *pGBKT7-Vps1 GED*
KKY 1480	This study	KKY 1255 *pGADT7-Vps22* (1-100aa)

Table 1. Yeast Strains Used in My Study

Strain Number	Source	Genotype
KKY 1482	This study	KKY 1480 x KKY 1275
KKY 1483	This study	KKY 1480 x KKY 1438
KKY 1484	This study	KKY 1480 x KKY 1439
KKY 1485	This study	KKY 1480 x KKY 1440
KKY 1486	This study	KKY 1481 x KKY 1275
KKY 1487	This study	KKY 1481 x KKY 1438
KKY 1488	This study	KKY 1481 x KKY 1439
KKY 1489	This study	KKY 1481 x KKY 1440
KKY 1494	This study	KKY 002 pRS314-mRFP-Cps1
KKY 1495	This study	KKY 352 pRS314-mRFP-Cps1
KKY 1496	This study	KKY 1034 pRS314-mRFP-Cps1
KKY 1497	This study	KKY 250 pRS314-mRFP-Cps1
KKY 1498	This study	KKY 251 pRS314-mRFP-Cps1
KKY 1499	This study	KKY 252 pRS314-mRFP-Cps1
KKY 1500	This study	KKY 270 pRS314-mRFP-Cps1
KKY 1515	This study	KKY 1255 pGADT7-Spa2
KKY 1519	This study	KKY 866 pRS314-mRFP-Cps1
KKY 1520	This study	KKY 248 pRS314-mRFP-Cps1
KKY 1521	This study	KKY 249 pRS314-mRFP-Cps1
KKY 1522	This study	KKY 1061 pRS314-mRFP-Cps1
KKY 1523	This study	KKY 1062 pRS314-mRFP-Cps1
KKY 1541	This study	KKY 1255 pGADT7-Ste24
KKY 1542	This study	KKY 1255 pGADT7-Vps36 (1-236aa)
KKY 1543	This study	KKY 1255 pGADT7-Vps36 (236-566aa)
KKY 1544	This study	KKY 1542 x KKY 1275
KKY 1545	This study	KKY 1542 x KKY 1438
KKY 1546	This study	KKY 1542 x KKY 1439
KKY 1547	This study	KKY 1542 x KKY 1440
KKY 1548	This study	KKY 1543 x KKY 1275
KKY 1549	This study	KKY 1543 x KKY 1438
KKY 1550	This study	KKY 1543 x KKY 1439
KKY 1551	This study	KKY 1543 x KKY 1440
KKY 1587	This study	KKY 1275 x KKY 1515
KKY 1588	This study	KKY 1275 x KKY 1541
KKY 1623	This study	KKY 352 pRS315-GFP-Vps1
KKY 1648	This study	KKY 1494 pRS315-Vps1
KKY 1649	This study	KKY 1495 pRS315-Vps1
KKY 1650	This study	KKY 1520 pRS314-Vps1
KKY 1651	This study	KKY 1521 pRS314-Vps1
KKY 1652	This study	KKY 1497 pRS314-Vps1
KKY 1653	This study	KKY 1498 pRS314-Vps1
KKY 1654	This study	KKY 1499 pRS314-Vps1
KKY 1655	This study	KKY 1500 pRS315-Vps1
KKY 1656	This study	KKY 1496 pRS315-Vps1
KKY 1657	This study	KKY 1519 pRS315-Vps1
KKY 1658	This study	KKY 1522 pRS315-Vps1

Table 1.Yeast Strains Used in My Study

Strain Number	Source	Genotype
KKY 1706	This study	KKY 343 pRS314-GFP-Pep12, pRS316-mRFP-Vps36
KKY 1707	This study	KKY 352 pRS314-GFP-Pep12, pRS316-mRFP-Vps22
KKY 1708	This study	KKY 352 pRS314-GFP-Pep12, pRS316-mRFP-Vps36
KKY 1709	This study	KKY 343 pRS315-GFP-Vps1, pRS316-mRFP-Vps22
KKY 1710	This study	KKY 343 pRS315-GFP-Vps1, pRS316-mRFP-Vps36
KKY 1711	This study	KKY 352 pRS315-GFP-Vps1 pRS316-mRFP-Vps22
KKY 1712	This study	KKY 352 pRS315-GFP-Vps1 pRS316-mRFP-Vps36

Table 2. Bacterial Plasmids Used in My Study

Plasmid Number	Source	Plasmid
KKD99	Clontech	pGBKT7
KKD100	This study	pGBKT7-p53
KKD101	This study	pGBKT7-Lamin
KKD63	(Furuta et al., 2007)	*pRS416 Pep12*-GFP
KKD69	(Furuta et al., 2007)	pKT1566 *Tlg1-GFP*
KKD79	This study	*pGBKT7-Vps1*
KKD83	Clontech	*pGADT7*
KKD85	This study	*pGADT7*-SV40 T antigen
KKD94	Clontech	*pRS314*
KKD95	Clontech	*pRS315*
KKD96	Clontech	*pRS316*
KKD134	This study	*pGBKT7-Vps1* GTPase (1-340)
KKD130	This study	*pGBKT7-Vps1* GED (615-704)
KKD128	This study	*pGBKT7-Vps1* Middle (341-614)
KKD143	(Obara et al., 2013)	*p416 mRFP-CPS1*
KKD160	This study	*pGADT7-Vps22* (1-100)
KKD161	This study	*pGADT7-Vps22* (80-233)
KKD172	This study	*pGADT7-Vps36* (1-236)
KKD173	This study	*pGADT7-Vps36* (236-566)
KKD190	This study	*p416 mRFP-Vps1*
KKD193	This study	*pGADT7-Spa2* C-term (825-1467)
KKD 210	This study	*pGADT7-Ste24* C-term (398-454)
KKD 277	This study	*pRS315-Vps1*
KKD 280	This study	*pRS315-GFP-Vps1*
KKD 285	This study	*pRS314-VPS1*
KKD 306	This study	*pRS314-Vps36-mRFP*
KKD 307	This study	*pRS314-Vps22-mRFP*

RESULTS

Vps1 Physically Interacts with ESCRT-II Subunits

Our lab has recently revealed that Vps1 can physically interact with ESCRT-II and ESCRT-III subunits (unpublished data). To further explore these interactions, I have performed a yeast-two hybrid assay between Vps1 and ESCRT-II subunits, Vps22 and Vps36. Yeast strains expressing Vps1 fragments, such as GTPase (1-340aa), Middle (340-614aa), and GED (614-704aa) domains, were cloned into bait vector (pGBKT7) and mated with yeast strains expressing the N-terminal 100 aa of Vps22, the C-terminal 153 aa of Vps22 (80-233aa), the N-terminal 236 aa of Vps36, or the C-terminal 330 aa of Vps36 (236-566aa). My results showed that all Vps1 domains are capable of interacting with the N-terminal fragment of Vps22, but not the C-terminal fragment (Figure 4A and 4B). However, Vps1 was able to interact with both the N- and C-terminal fragments of Vps36 (Figure 4C and 4D).

Vps1 and ESCRT-II Subunits Colocalize at the Endosome

Both ESCRT and Vps1 have been previously shown to function at the endosome (Hayden et al., 2013; Hurley and Emr, 2006). Therefore, I reasoned that Vps1 and ESCRT-II subunits, Vps22 and Vps36, colocalize at the endosome. For this, I first constructed yeast strains expressing GFP-fused Pep12 (GFP-Pep12), as an endosome marker, as previously described (Gerrard et al., 2000). Then, N- or C-terminal mRFP fused proteins, including mRFP-Vps1, Vps22-mRFP, and Vps36-mRFP, were expressed along with GFP-Pep12. My results showed that mRFP-Vps1, Vps22-mRFP, and Vps36-

mRFP partially localize to the endosomal marker, GFP-Pep12 (Figure 5A and 5B). In particular, loss of Vps1 has no effect on the subcellular localization of Vps22 and Vps36 (Figure 5B), suggesting the endosomal targeting of these ESCRT II components does not require the presence of Vps1 at the endosome. Similarly, I expressed mRFP-Vps1 with the early endosome marker Tlg1-GFP. It was found that 45±4 % of mRFP-Vps1 puncta colocalized with those of Tlg1-GFP, while in *vps22*Δ the colocalization level was decreased to 34±8 % ($p = 0.09$). Cells lacking Vps36 reveals 53±6.6 % of colocalization between Vps1 and Tlg1 ($p = 0.17$) (Figure 5C). Therefore, the reduction of levels of Vps1 colocalization in *vps22*Δ indicates that Vps22 plays a role in Vps1 recruitment to the Tlg1-carrying endosome. Proteins that function together at the same subcellular location colocalize with each other. In order to test the idea of tentative colocalization of Vps1 with Vps22 and Vps36 at the endosome, I engineered yeast cells to coexpress GFP-Vps1 and Vps22-mRFP or Vps36-mRFP, and found that GFP-Vps1 partially colocalizes with both Vps22-mRFP and Vps36-mRFP (Figure 5D).

Loss of Vps1 or Inactivation of the GTPase Activity of Vps1 Resulted in Cps1 Mistargeting

The physical interaction and colocalization of Vps1 with Vps22 and Vps36, as well as the intrinsic membrane remodeling activity of Vps1 (Williams and Kim, 2014), strongly indicate a functional implication of Vps1 in the process of cargo sorting during formation of the multivesicular body. My strategy to test this idea was to monitor distribution patterns of the cargo Cps1 in *vps1* mutant cells. Cps1 is a vacuolar transmembrane carboxypeptidase that is synthesized in the ER and targeted to the Golgi

complex before reaching the endosome, where Cps1 is sorted into ILVs with the aid of the ESCRT system (Cowles et al., 1997; Odorizzi et al., 2003). mRFP-fused Cps1 was evenly distributed in the vacuole lumen in 90.6% of wild type cells (Figure 6A), indicating a proper sorting of Cps1 into ILVs at the late endosome prior to the fusion of late endosomes with the vacuole. In contrast, only 45.9% of *vps1*Δ cells displayed normal phenotypes, and the rest of the mutant cells exhibited a mutant phenotype of a stronger concentration of mRFP-Cps1 at the rim of the vacuole (Figure 6A and 6B), as the case for ESCRT mutant cells; 85.8% of *vps*22Δ , 91% of *vps*36Δ, 90.4% of *vps*2Δ, and 91.6% of *vps*24Δ cells exhibited Cps1 mislocalization at the rim of the vacuole (Figure 6A and 6B). The reintroduction of Vps1 in *vps1*Δ cells rescued the abnormal mRFP-Cps1 distribution pattern (Figure 6A and 6B), suggesting the Cps1 localization defect observed in Vps1-lacking cells was the direct cause of the loss of Vps1. Vps1 acts through the binding and hydrolysis of GTP in its active site (Yu and Cai, 2004). Three residues of Vps1 implicated in the GTP binding/hydrolysis are K42, S43, and G315 (Yu and Cai, 2004). Vps1 point mutant cells expressing $vps1^{K42E}$, $vps1^{S43N}$, or $vps1^{G315D}$ were found to display similar levels of the Cps1 mistargeting defect as compared with cells deficient in Vps1 (Figure 6A and 6B), pointing to the significance of the GTPase activity of Vps1 on Cps1 targeting to the vacuole.

Next, I set out to test whether Vps1 functions redundantly with or downstream of ESCRT components, for which the full-length Vps1 was overexpressed in cells lacking a component of ESCRT II and III (*vps*22Δ , *vps*36Δ, *vps*2Δ, or *vps*24Δ). It was found that Vps1 overexpression was not capable of rescuing the Cps1 mislocalization in *vps22*Δ and *vps24*Δ cells, but in *vps2*Δ (p=0.090) and *vps36*Δ cells (p=0.076), I observed a partial

rescue of severe Cps1 targeting defects (Figure 6B). Together, these results suggest no noticeable functional connection between Vps1 and Vps22 and Vps24, but Vps1 appears to play modestly redundant roles of Vps2 and Vps36 at the endosome for Cps1 targeting.

Yeast-Two Hybrid Library Screen for Vps1 Binding Partners

In my search for novel Vps1 binding partners, I performed a yeast two-hybrid library screen using Clontech's Make Your Own "Mate & Plate" Library System (Cat. No. 630490). For this, full length *VPS1* sequence was cloned into BD (DNA Binding Domain, pGBKT7) vector to screen a yeast cDNA library fused to gal-4 AD (Activation Domain, pGADT7-rec) vector. My initial screen yielded sixty-nine positive colonies on Triple Drop Out (TDO) medium, which were picked and patched onto new TDO medium (Fig. 7A). Upon replica plating onto a more stringent Quadruple Drop Out (QDO) medium, sixty-four colonies grew (Fig. 7B). Fifty-eight colonies grew and produced blue color when replica plated onto Double Drop Out medium with X-alpha-gal and aureobasidin (DDO/X/A) (Fig. 7C). The isolated prey vectors from the positive colonies grown on these stringent tests were analyzed by comparing their cDNA inserts with the BLAST (Basic Local alignment Search Tool).

After excluding both the cloned DNA sequences originated from rRNA species and low-purity sequencing errors, the sequencing analysis revealed seventeen novel binding partners for Vps1 (Table 3). These partners appear to be involved in a wide range of cellular processes, including stress responses, signaling transduction pathways, ribosomal activities, and mating processes. For example, Fes1 and Pre10 are implicated in targeting misfolded proteins for ubiquitination in different stress responses (Gowda et

al., 2013; Janse et al., 2004), while Pbs2 is involved in signal transduction (Zarrinpar et al., 2004). Eight proteins (Drs1, Pxr1, YLR154C, Rps1B, RPL18A, RPL26B, RNH203, and YDR341C) are involved in ribosome-associated activity. Spa2, Ste24 and SCW4 localizes to the plasma and ER membranes and are all implicated in the yeast mating process (Cappellaro et al., 1998; Meissner et al., 2010; Noma et al., 2005).

In order to validate the results, I selected two Prey proteins and tested their ability to interact with Vps1: Spa2, a cytoplasmic protein, and Ste24, an integral protein. Though previous studies have not linked Vps1 and Spa2, Ste24 has been shown to genetically interact with Vps1 (Hoppins et al., 2011; Jonikas et al., 2009; Surma et al., 2013). Sequencing analysis from my library screen showed that the C-terminal ends of Spa2 and Ste24 were inserted into the library vector. For one-on-one interaction study, pGADT7 vector was engineered to contain the C-terminal 642 aa of Spa2 (825-1467aa) or the C-terminal 56 aa of Ste24 (398-453aa), and then the yeast strains expressing the recombinant protein fragments were mated with the strain carrying Vps1-BD bait vector. The mated cells were spotted on TDO medium in serial dilutions (Figure 7D). Strains expressing both prey and bait vectors grew on TDO medium, but not on QDO medium (Data not shown), suggesting Spa2 and Ste24 appear to interact with Vps1, but at lower efficiency than previously tested in the library screen (Fig. 7A-C). One possible explanation for a weak binding between Vps1 and these binding partners would be that the cloned C-terminal fragments of Spa2 and Ste24 used in this one-on-one two-hybrid assay are larger than those cloned in the library vectors, and thus the increase in peptide size may have altered the conformation of these proteins.

DISCUSSION

The ESCRT complex collectively recognizes ubiquitinated cargo and deforms the endosomal membrane locally to generate ILVs into which cargo is sequestered (Woodman, 2016). An emerging concept is that proteins implicated in a similar function act together by forming a multiprotein complex at the designated subcellular compartment where they function. My study for the first time provides evidence that components of ESCRT-II and -III are physically associated with another membrane-remodelling protein, Vps1, at the endosome and that Vps1 shares a redundant role with these components, including Vps2 and Vps22, for efficient sorting of the cargo Cps1 into ILVs. At the moment, the biochemical targeting mechanism of Vps1 to the endosome has not been revealed, but a recent lipid binding preference test exhibited that Vps1 strongly interacts with PI3P, which is highly enriched in the endosome (Smaczynska-de et al., 2015), pointing to a lipid-binding ability of Vps1 that may facilitate its recruitment to the endosome. In light of the finding that multiple components of the ESCRT system, including Vps22, Vps36, Vps24, and Vps2 bind to Vps1, one can postulate that these protein factors may contribute to the recruitment of Vps1 onto the endosomal membrane. However, my results show that a knock out of *Vps*36 does not significantly affect Vps1 targeting to the endosome. Based on this observation, it is plausible to propose the recruitment of Vps1 to endosome occurs independent of the ESCRT system and that the significance of their interaction occurs downstream or in a yet identified process. Regardless, the precise temporal recruitment mechanism of Vps1 to the endosome awaits to be explored.

Structurally, Vps22 and Vps36 interact together to form one lobe of ESCRT-II's three lobed structure (Teo et al., 2004a). Both Vps22 and Vps36 contain Winged-Helix 1 (WH1) and WH2, which are essential for binding to Vps25 and forming ESCRT-II's second and third lobes (Im and Hurley, 2008). Because Vps1 does not interact with Vps25, it is likely that Vps1 is associated with the Vps22/Vps36 stem or lobe, which protrudes away from the body of the ESCRT-II complex. At the stem, the N-terminal Helical Domain (HD) of Vps22 and the N-terminal GRAM-Like Ubiquitin-binding in EAP45 (GLUE) domain of Vps36 are exposed to the solution. According to my yeast two-hybrid experiments, Vps1 appears to interact with these HD and GLUE domains. The GLUE domain of ESCRT-II is known to be one such hub that can recognize endosomal membranes, ubiquitinated cargo and ESCRT-I simultaneously (Gill et al., 2007). Moreover, the HD region of Vps22 plays an important role for Cps1 sorting (Im and Hurley, 2008). Taken together, it appears that Vps1 is spatially located at a "hot spot" that is essential for the function of ESCRT-II (Figure 8). Yet the physiological relevance of the interaction is not clear. It is speculated that Vps1 aids in the cargo sorting process, as a partner of the multiprotein complex ESCRT-II, because loss of Vps1 leads to a noticeable Cps1 mislocalization that might have been caused by a sorting defect at the endosome. As all Vps1 point mutants crippled in its GTP-binding/hydrolysis exhibited Cps1 sorting defects, reminiscent of the defects caused by the loss of Vps1, one can suggest that both the physical presence of Vps1 at the "hot spot" and its GTPase activity are essential for Vps1 function in Cps1 sorting. A tentative role of Vps1, namely Cps1 sorting at the endosome, has been indirectly supported by the observation that loss of Vps1 led to a reduction in the number of ILVs (~50% of Wild type cells) whose size

appears to increase by about 1.2 times (Chi et al., 2014). Tying this result with my Cps1 sorting defect data in *vps1* mutant cells, it is plausible to hypothesize that Vps1 may play a direct role in ILV formation, through its *bona fide* membrane-remodeling activities, as reported previously (Smaczynska-de et al., 2010). Retrospectively, *vps1* mutants displayed a severe defect in proper targeting of Ste2, a transmembrane cargo that is ubiquitinated at the plasma membrane and targeted to the endosome and then to the vacuole in response to the yeast pheromone (Hayden et al., 2013). It may be that the defect of Ste2 accumulation at the late endosome in *vps1* mutant cells is accounted by a sorting defect of Ste2 and/or a defect in the formation of ILVs. Given that Vps1 is heavily implicated in homotypic vacuole fusion by facilitating the formation of SNARE and HOPS complex between approaching vacuoles (Alpadi et al., 2013; Kulkarni et al., 2014a), one more speculative explanation for Cps1 and Ste2 mistargeting in *vps1* mutants would be a defect in the fusion of late endosomes with the vacuole.

Vps1's versatility as a membrane-remodeling protein at multiple organelles has led me to explore its binding partners. Vps1's ability to work at different membranes may be attributed to its ability to interact with a variety of proteins. My yeast-two hybrid screen revealed seventeen novel binding partners. Among these interactions, I noticed several clusters of proteins with similar functions to Vps1. In particular, Vps1 interaction with Spa2 and Ste24 may create new insights into possible roles for Vps1. For example, given that Spa2, a polarisome subunit, (Snyder, 1989) and Vps1 are implicated in actin organization (Virag and Harris, 2006; Yu and Cai, 2004), it is possible that Vps1 works together with Spa2 synergistically or redundantly to help reorganize the actin cytoskeleton for cellular polarization. Importantly, recent studies demonstrated that Vps1

interacts genetically with Ste24, an ER transmembrane protein with the C-terminal exposed to the cytosol (Hoppins et al., 2011; Jonikas et al., 2009; Pryor et al., 2013; Surma et al., 2013). In light of finding physical interaction between Vps1 and the C-terminal fragment of Ste24, I speculate that Vps1 can be targeted to the periphery ER, but this speculative idea awaits further testing.

Previously, *vps1*Δ cells have been shown to exhibit abnormal budding and altered chitin deposition (Yu and Cai, 2004). However, the molecular details behind this defect had not been documented. According to my Vps1 interaction results, Vps1 physically interacts with proteins involved in the recruitment (Spa2), maintenance (Scw4), and targeting (Ste24) of chitin synthases (Figure 9), suggesting a model linking Vps1 to multiple factors involved in chitin distribution for cellular budding. In this model, I propose that when induced by mating factors, the Spa2-containing polarisome localizes to the nascent bud to aid in actin reorganization and cellular signaling, which promotes the recruitment of new cell materials (Sheu et al., 1998; Snyder, 1989). In response to mating signaling, chitin synthase III (Chs3), a major player in chitin production, is delivered to the plasma membrane from the ER by passing the *trans*-Golgi network (Starr et al., 2012). I speculate that Ste24 and Vps1 work together at the ER, as explained above, to sort and aid in fission of Chs3-containing vesicles. Upon arriving at the plasma membrane, Scw4, a soluble cell wall glucanase, is then involved in maintaining the integrity of the cell wall (Sestak et al., 2004). Taken together, it is likely that Vps1 is involved in several steps of the Chs3 trafficking pathway. However, additional studies are required to further validate these ideas.

In summary, my results have provided evidence for Vps1's role with ESCRT at the endosome and in chitin synthesis during cellular budding. It is notable to mention that in mammalian systems, certain ESCRT complexes are implicated in cytokinesis. However, this is yet to be seen in yeast. Considering dynamin and ESCRT's work at the mammalian plasma membrane, it is not unrealistic to hypothesize a scenario where Vps1, Spa2, and ESCRT work together at the polarized bud to aid in cellular division. Future studies in this field will look towards elucidating the precise mechanism for each of these functions. *In vitro* models using liposomes resembling yeast plasma membrane or endosomes will allow us to narrow down the efficiency of each component during membrane remodeling. Furthermore, it would be beneficial to narrow down the residues involved in these interactions. This information will provide a greater range of tools for our study from predictive modeling to constructing point mutants specific to our experiment.

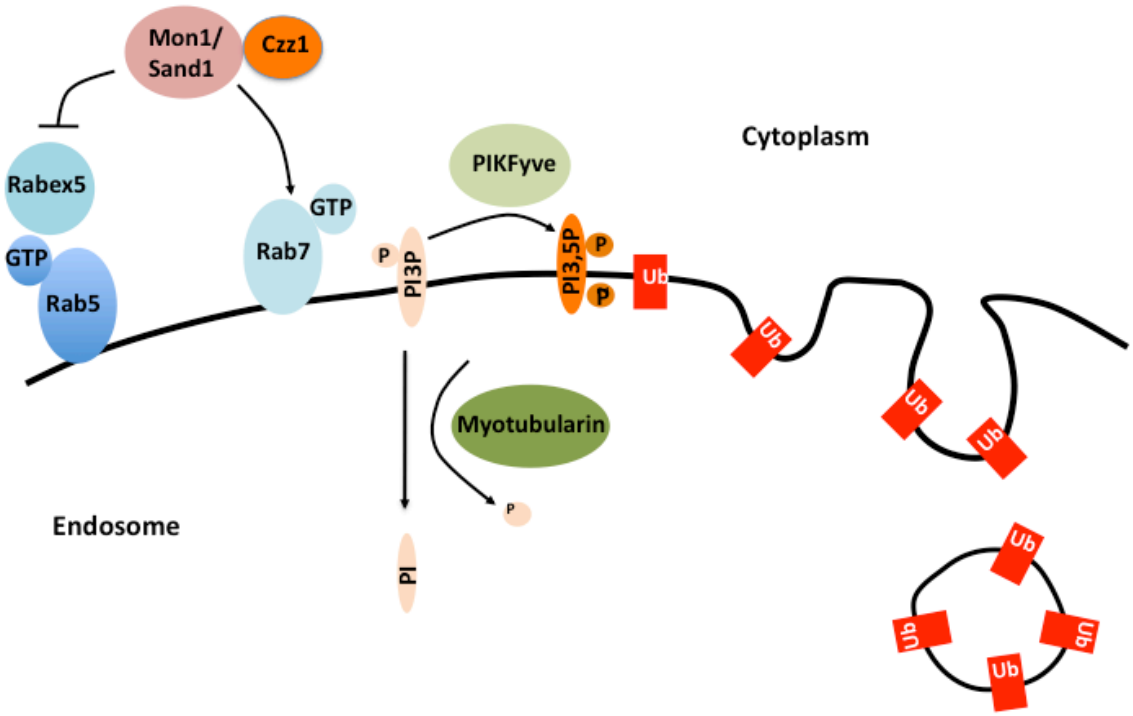

Figure 1. Endosome Maturation. A series of changes occur at the early endosomal membrane, which leads to the formation of the late endosome. Of these, a Rab switch occurs. The Mon1/Sand1 and Czz1 complex displaces the Rabex5 and helps recruit and activate Rab7 to the endosome. Additionally, the PI3P-dominant EE shifts towards a $PI3,5P_2$-dominant LE. This event can take place through PI3P phosphorylation by PIKfyve or dephosphorylation by myotubularin and recycling. The third major phenotypic change is the appearance of ILVs. These vesicles are formed through the ESCRT complex and contain sorted cargo intended for the vacuolar lumen.

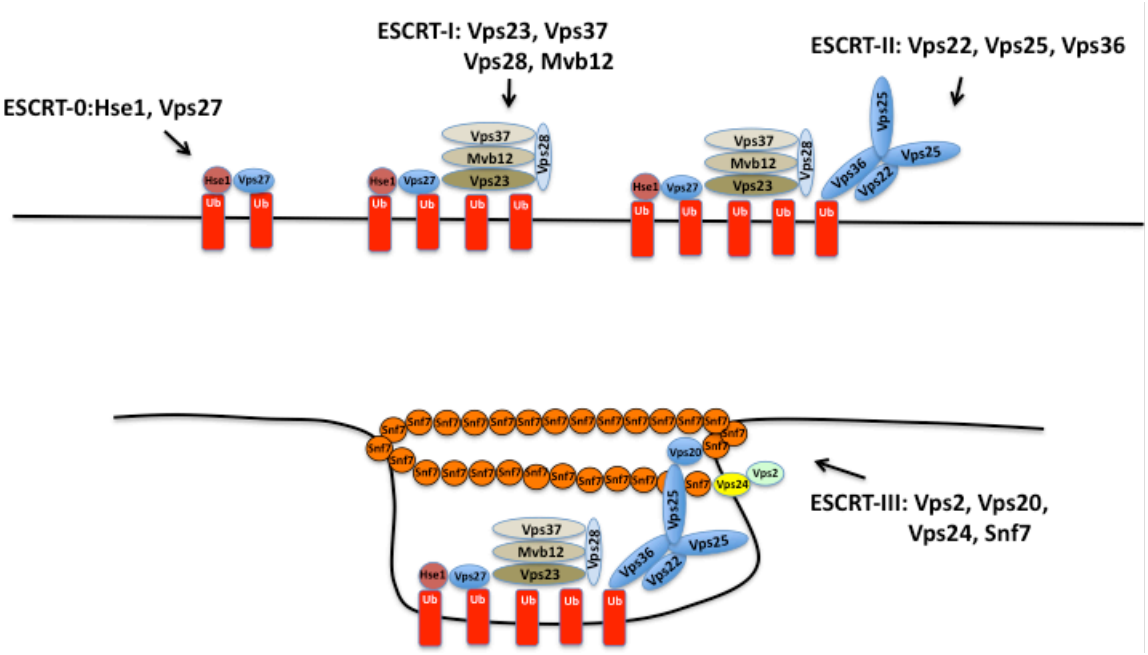

Figure 2. Intralumenal Vesicle formation by ESCRT. ESCRT complexes are recruited in a sequential manner to sort ubiquitinated cargo into ILVs. ESCRT-0, -I,-II are capable of interacting with ubiquitin. Additionally, interaction between each sequential pairs allows localization of the complexes with their cargo. The ESCRT-III complex is recruited and activated by ESCRT-II and is primarily involved in the fission of the ILV.

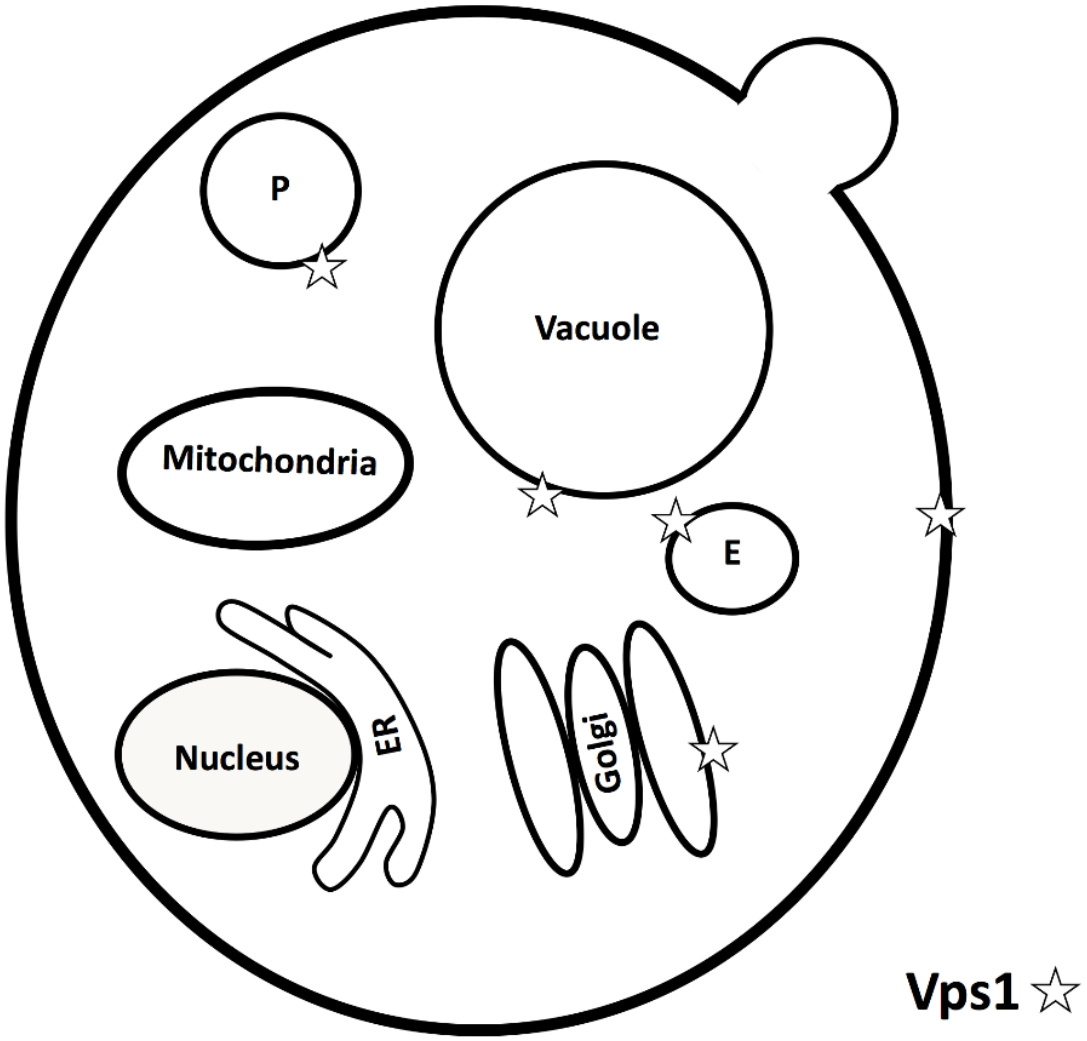

Figure 3. Localization of Vps1 in *S. cerevisiae*. Dynamin-like protein, Vps1 is a cytoplasmic protein that is targeted to the periphery of various membrane-bound organelles, including the peroxisome (P), endosome (E), Golgi, vacuole, and the plasma membrane. Vps1 is implicated in membrane remodeling activity, such as membrane tubulation and scission of vesicles emerging from these organelles. Vps1 locations are indicated by stars.

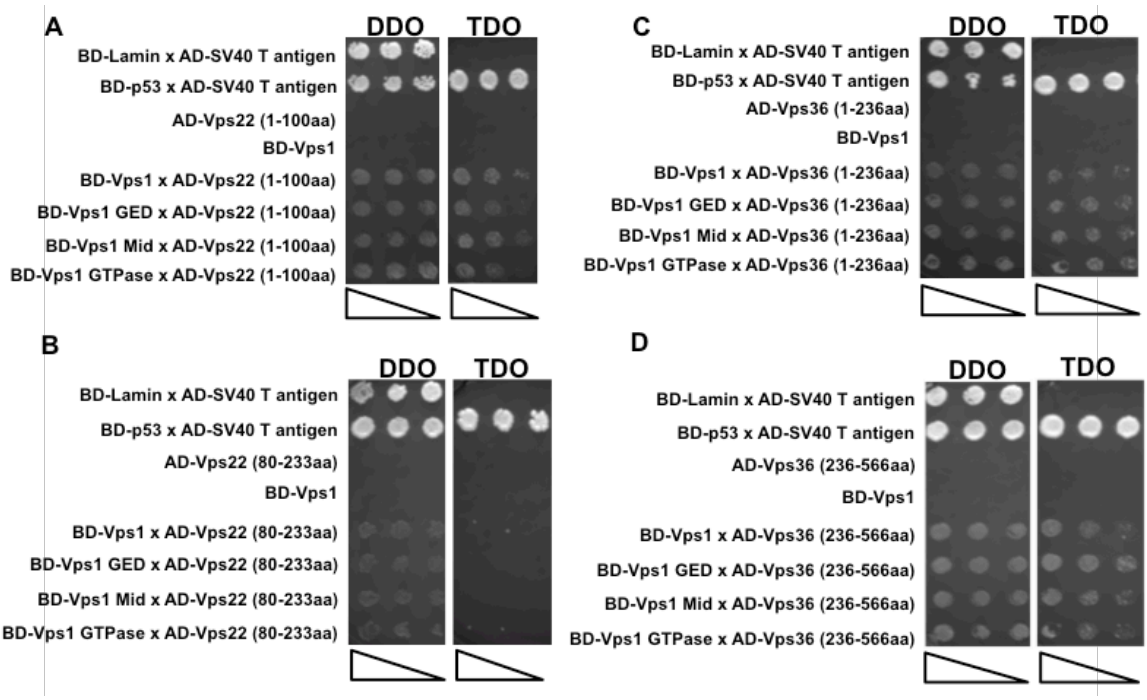

Figure 4. Mapping of domains of Vps22 and Vps36 required for Vps1 binding. Cells harboring Vps1 full length (1-704aa) or a domain of Vps1 (GTPase (1-340aa), Middle (340-614aa), and GED (614-704aa)) were mated with cells expressing 2A) the N-terminal Vps22 (1-100aa), 2B) the C-terminal Vps22 (80-233aa), 2C) the N-terminal Vps36 (1-236aa), or 2D) the C-terminal Vps36 (236-566aa). A spotting assay was performed by serially diluting yeast cells by a factor of 3, followed by plating the cells on selective media, such as DDO and TDO. Cell concentration gradients are indicated by triangles with the tip pointing toward lower concentration.

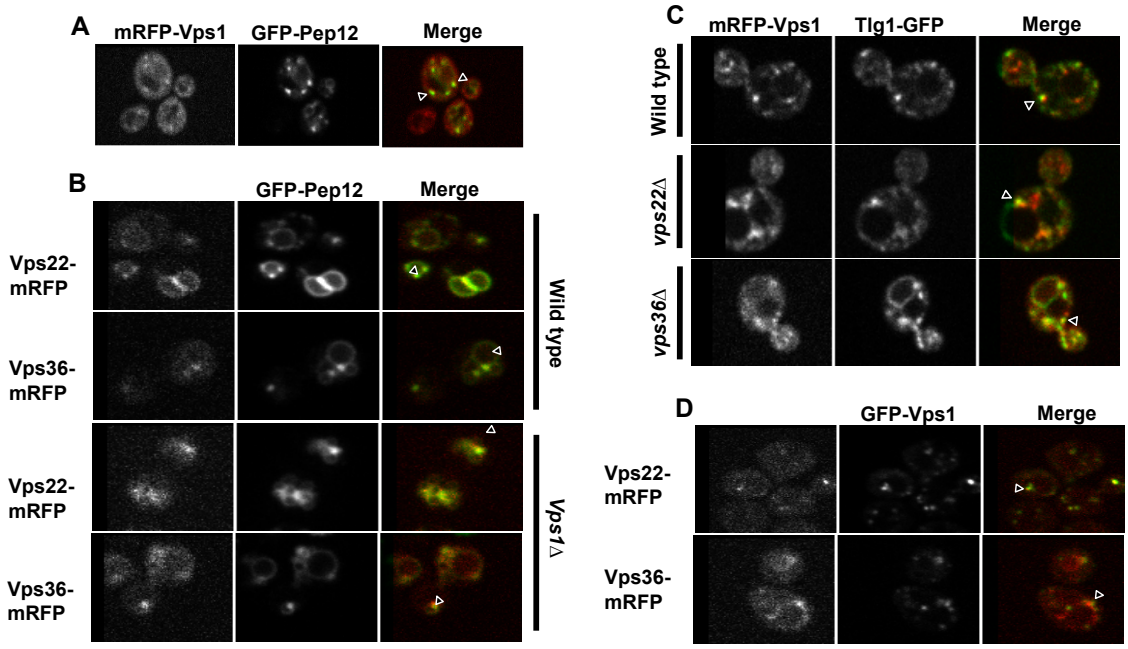

Figure 5. Vps1 and ESCRT-II Subunits Localize to the Endosome. A) mRFP-Vps1 was coexpressed with GFP-Pep12, a late endosomal marker, in a *vps1*Δ background. Arrowheads indicate colocalization between mRFP-Vps1 and GFP-Pep12. B) mRFP-fused ESCRT-II subunits, Vps22-mRFP and Vps36-mRFP, colocalize to fluorescent puncta containing GFP-Pep12 in a wild type background. Additionally, cells deficient in Vps1 does not appear to display a defective phenotype in the targeting of Vps22 and Vps36 to the endosome. C) mRFP-Vps1 and Tlg1-GFP were expressed in WT, *vps22*Δ, and *vps36*Δ background. D) GFP-Vps1 and Vps22-mRFP or Vps36-mRFP were simultaneously expressed in *vps1*Δ cells. Points of colocalization are indicated by arrowheads.

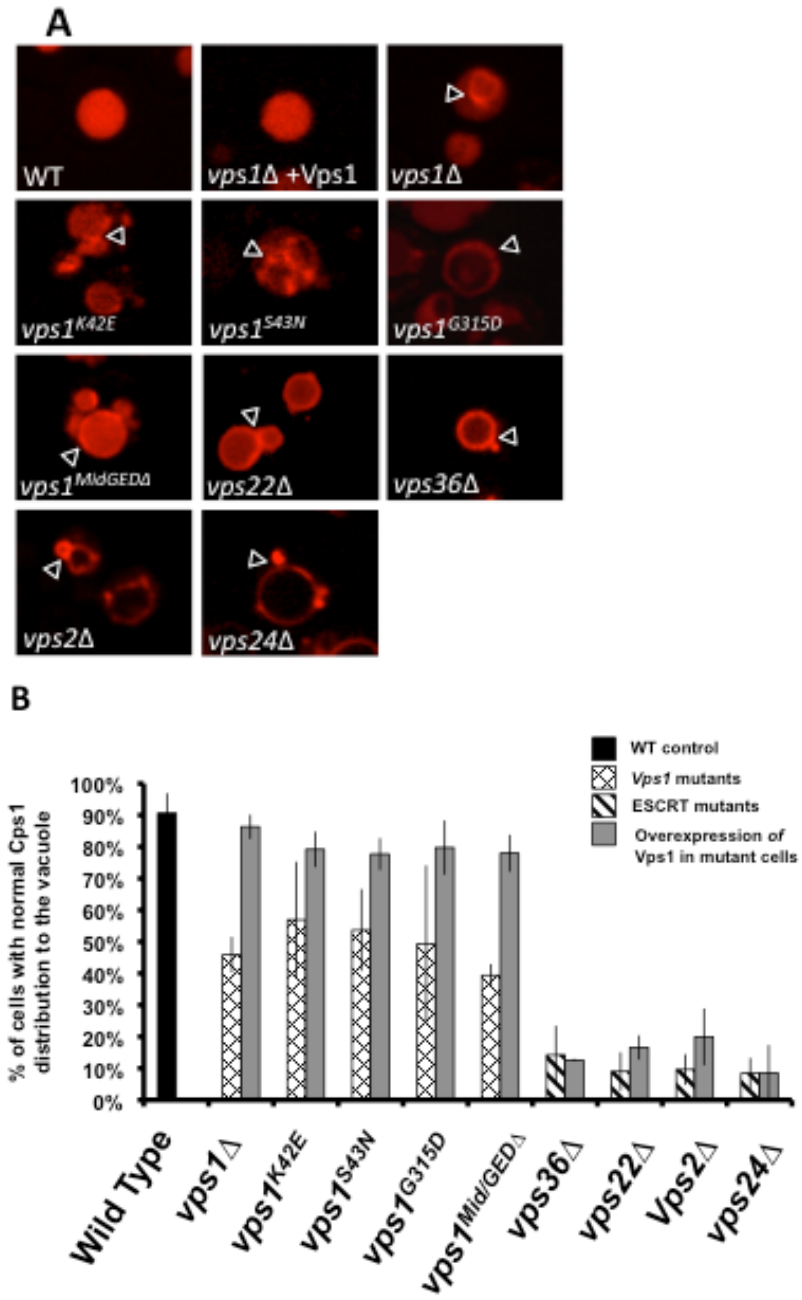

Figure 6. mRFP-Cps1 is Mistargeted in Vps1 and ESCRT-II and –III Mutant Cells. A) mRFP-Cps1 was expressed in wild type, *vps1*Δ, 3 *vps1* GTPase point mutants, a *vps1* middle and GED truncation mutant, and ESCRT-II/–III subunit knockout strains. Wild type phenotype was represented by an even stain of mRFP-Cps1 in the lumen of the vacuole. Mutant cells exhibit an accumulation of mRFP-Cps1 at the rim of the vacuole in comparison to its lumen. Arrowheads indicate points of abnormal accumulation of mRFP-Cps1. B) Vps1 was overexpressed in the mutant cells above to explore the possibility that Vps1 could functionally restore Cps1 missorting. Student's T-test indicated that the reintroduction of Vps1 in *vps1*Δ, $vps1^{S43N}$, and $vps1^{Mid/GED\Delta}$ cells resulted in a statistically significant recovery (p-value <0.05). While *vps2*Δ and *vps36*Δ had marginally significant recovery (p-value <0.1). s

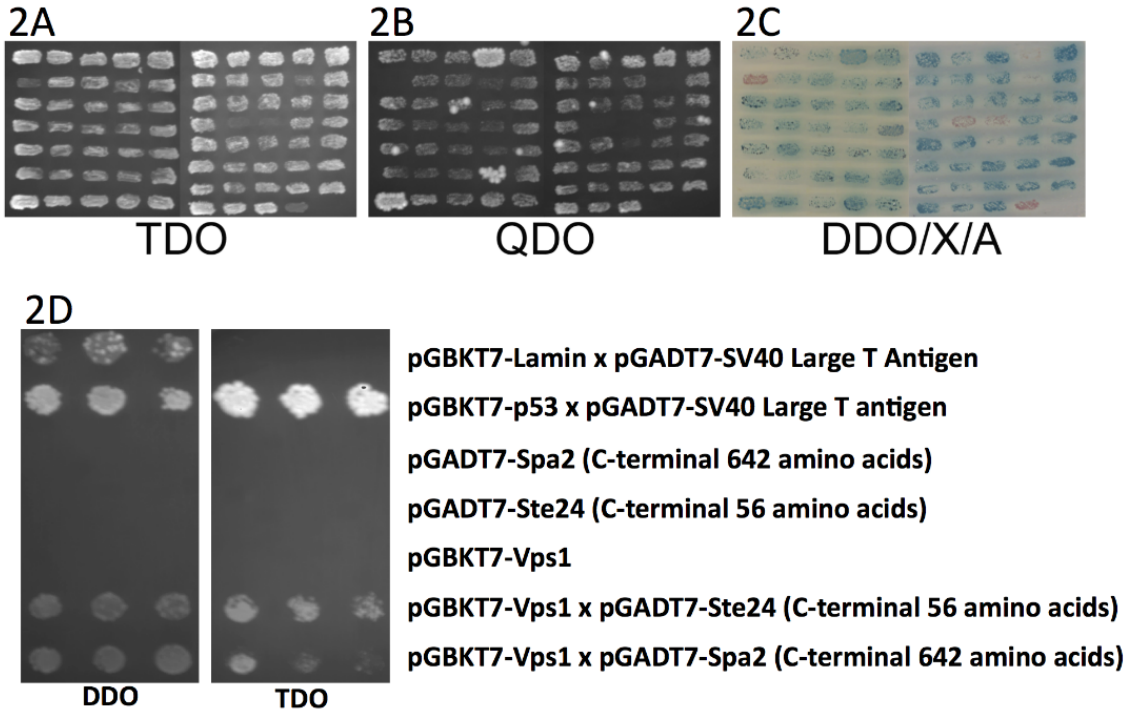

Figure 7. Yeast Two-Hybrid Genome-Wide Screen for Searching Vps1 Binding Partners in *S. cerevisiae*. 7A-C. The harvested prey library pool (pGADT7-Rec cDNA) was mated with the bait strain (pGBKT7-Vps1), and the mated diploid cells were plated onto TDO (2A), QDO (2B), and DDO/X/A (2C). 2D. Verification of my library assay by one-on-one yeast two-hybrid assay. For a positive control, cells expressing BD-p53 and AD-SV40 large T antigen were utilized; p53 was inserted into the bait vector (pGBKT7) and SV40 large T antigen into the prey vector (pGADT7). Cells expressing BD-Lamin and AD-SV40 large T antigen, which do not bind to each other, served as the negative control. Following the same method, the full length of *VPS1* was inserted into the bait vector, and the indicated C-terminal regions of Spa2 and Ste24 were cloned into the prey vector. Diploid cells harboring both the bait and Prey vectors were plated on DDO (Double Drop Out) and TDO (SD/-Leu/-Trp/-His). Only positive control strain and the strains containing both the bait and Prey grew on TDO medium, indicating that Vps1 interacts with Ste24 and Spa2.

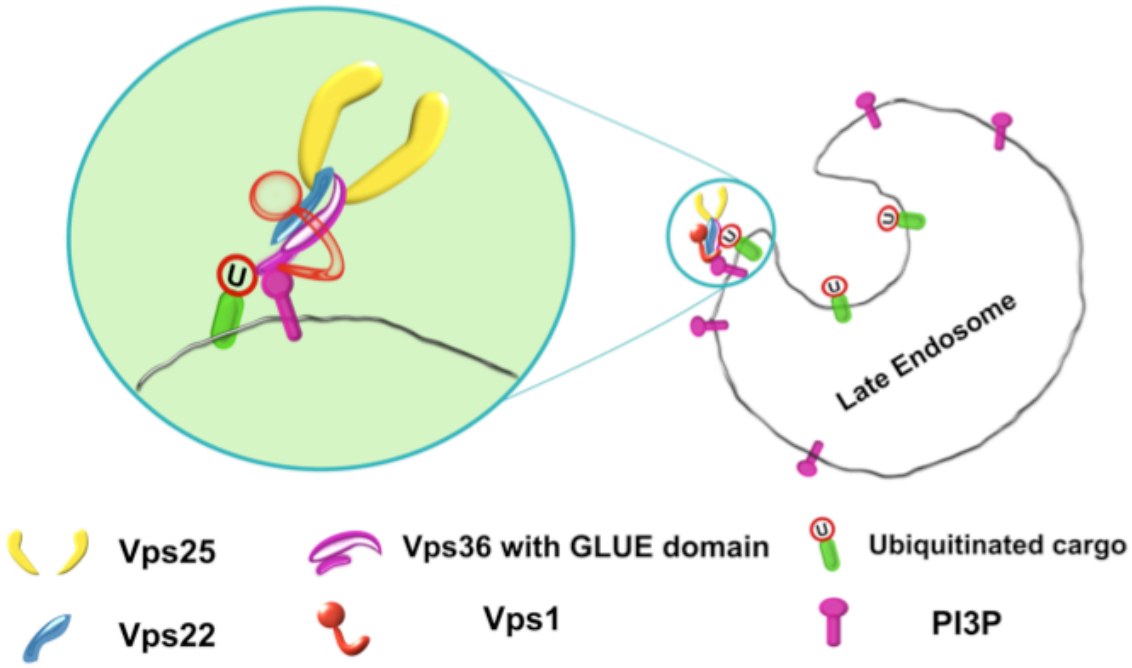

Figure 8. A Potential Model of Vps1 and ESCRT-II Interaction at the Endosome. ESCRT-II localization to the endosome is mediated by the N-terminal region of its Vps22/Vps36 lobe. The tip or "hot spot" of lobe contains the GLUE domain of Vps36, which binds to ubiquitinated cargo and PI3P. The HD domain of Vps22 is also speculated to be a part of the "hot spot". Vps1 was added to the diagram, near the periphery of the tip of the lobe for it interacts with the N-terminal GLUE and HD domains of Vps36 and Vps22, respectively. Another rationale behind the inclusion of Vps1 at the "hot spot" is that Vps1localizes to the late endosome and interacts with PI3P in vitro (Hayden et al., 2013; Smaczynska-de et al., 2015). The ESCRT II-Vps1 complex may function together for cargo recognition and its subsequent sequestration into ILVs.

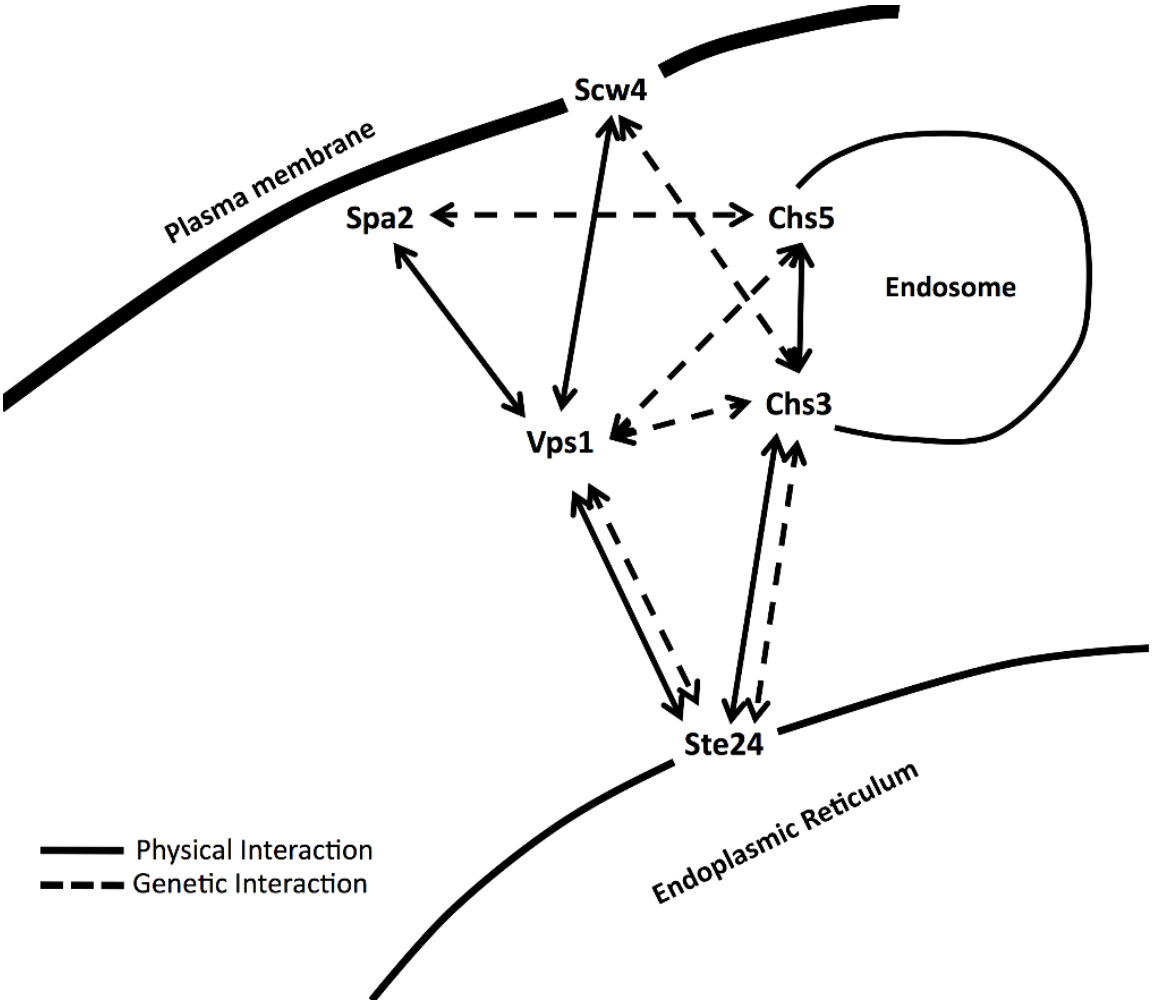

Figure 9. Interaction Mapping of Vps1 in Chitin Deposition. My results show that Vps1 physically interact with factors involved in mating induced budding; Spa2, Ste24, and Scw4 (see the main text). These proteins have all been implicated in targeting, recruiting, or maintaining chitin synthases (Chs3 and Chs5).

Table 3. Yeast Two Hybrid Screen of Vps1 Binding Partners

Gene Name	Accession Number	# of Clones	Function from Saccaromyces Genome Database
SPA2	X53731.1	1	A subunit of the polarisome; functions in actin cytoskeletal organization during polarized growth; acts as a scaffold for Mkk1p and Mpk1p cell wall integrity signaling components
STE24	U77137.1	1	Highly conserved zinc metalloprotease; functions in two steps of a-factor maturation, C-terminal CAAX proteolysis and the first step of N-terminal proteolytic processing
SCW4	Z73064.1	1	Cell wall protein with similarity to glucanases;
FES1	NM_001178449.3	2	Hsp70 nucleotide exchange factor
PRE10	Z75270.1	1	Alpha 7 subunit of the 20S proteasome
PBS2	Z49403.1	1	MAP kinase kinase of the HOG signaling pathway; mitophagy-specific regulator; plays a role in regulating Ty1 transposition
YNL054W-B	NM_001281536.1	1	Type B Gag-Pol protein; proteolytically processed to make the Gag, RT, PR, and IN proteins that are required for retrotransposition
DRS1	NM_001181828.1	2	Nucleolar DEAD-box protein required for ribosome assembly and function
PXR1	NM_001181409.1	1	Essential protein involved in rRNA and snoRNA maturation; a possible role in the negative regulation of telomerase
YLR154c/RNH203	Z73326.1	1	Ribonuclease H2 subunit; required for RNase H2 activity; role in the ribonucleotide excision repair
RPS1B	NM_001182422.1	1	Ribosomal protein 10 (rp10) of the small (40S) subunit
RPL18A	Z74862.1	1	Ribosomal 60S subunit protein L18A
RPL26B	Z72819.1	1	Ribosomal 60S subunit protein L26B

Table 3. Yeast Two Hybrid Screen of Vps1 Binding Partners

Gene Name	Accession Number	# of Clones	Function from Saccaromyces Genome Database
RNH203	Z73326.1	1	Ribonuclease H2 subunit; role in ribonucleotide excision repair; related to human AGS3 that causes Aicardi-Goutieres syndrome
YDR341C	NM_001180649.3	1	Arginyl-tRNA synthetase
YLR157C-C	Z73326.1	5	A protein of unknown function; Paralog of ASP3-2, implicated in asparagine catabolism
YLR179C	NM_001182066.1	1	A protein of unknown function with similarity to Tfs1p; transcription is activated by paralogous proteins Yrm1p and Yrr1p along with proteins involved in multidrug resistance

REFERENCES

Abutbul-Ionita, I., Rujiviphat, J., Nir, I., McQuibban, G.A., and Danino, D. (2012). Membrane tethering and nucleotide-dependent conformational changes drive mitochondrial genome maintenance (Mgm1) protein-mediated membrane fusion. J Biol Chem *287*, 36634-36638.

Alpadi, K., Kulkarni, A., Namjoshi, S., Srinivasan, S., Sippel, K.H., Ayscough, K., Zieger, M., Schmidt, A., Mayer, A., Evangelista, M.*, et al.* (2013). Dynamin-SNARE interactions control trans-SNARE formation in intracellular membrane fusion. Nat Commun *4*, 1704.

Anantharam, A., Bittner, M.A., Aikman, R.L., Stuenkel, E.L., Schmid, S.L., Axelrod, D., and Holz, R.W. (2011). A new role for the dynamin GTPase in the regulation of fusion pore expansion. Mol Biol Cell *22*, 1907-1918.

Arlt, H., Reggiori, F., and Ungermann, C. (2015). Retromer and the dynamin Vps1 cooperate in the retrieval of transmembrane proteins from vacuoles. J Cell Sci *128*, 645-655.

Babst, M., Katzmann, D.J., Snyder, W.B., Wendland, B., and Emr, S.D. (2002). Endosome-associated complex, ESCRT-II, recruits transport machinery for protein sorting at the multivesicular body. Dev Cell *3*, 283-289.

Bissig, C., and Gruenberg, J. (2013). Lipid sorting and multivesicular endosome biogenesis. Cold Spring Harb Perspect Biol *5*, a016816.

Blumer, J., Rey, J., Dehmelt, L., Mazel, T., Wu, Y.W., Bastiaens, P., Goody, R.S., and Itzen, A. (2013). RabGEFs are a major determinant for specific Rab membrane targeting. J Cell Biol *200*, 287-300.

Bonifacino, J.S., and Rojas, R. (2006). Retrograde transport from endosomes to the trans-Golgi network. Nat Rev Mol Cell Biol *7*, 568-579.

Boura, E., Rozycki, B., Herrick, D.Z., Chung, H.S., Vecer, J., Eaton, W.A., Cafiso, D.S., Hummer, G., and Hurley, J.H. (2011). Solution structure of the ESCRT-I complex by small-angle X-ray scattering, EPR, and FRET spectroscopy. Proc Natl Acad Sci U S A *108*, 9437-9442.

Bowers, K., Piper, S.C., Edeling, M.A., Gray, S.R., Owen, D.J., Lehner, P.J., and Luzio, J.P. (2006). Degradation of endocytosed epidermal growth factor and virally ubiquitinated major histocompatibility complex class I is independent of mammalian ESCRTII. J Biol Chem *281*, 5094-5105.

Cao, H., Garcia, F., and McNiven, M.A. (1998). Differential distribution of dynamin isoforms in mammalian cells. Mol Biol Cell *9*, 2595-2609.

Cappellaro, C., Mrsa, V., and Tanner, W. (1998). New potential cell wall glucanases of Saccharomyces cerevisiae and their involvement in mating. J Bacteriol *180*, 5030-5037.

Chappie, J.S., and Dyda, F. (2013). Building a fission machine--structural insights into dynamin assembly and activation. J Cell Sci *126*, 2773-2784.

Chappie, J.S., Mears, J.A., Fang, S., Leonard, M., Schmid, S.L., Milligan, R.A., Hinshaw, J.E., and Dyda, F. (2011). A pseudoatomic model of the dynamin polymer identifies a hydrolysis-dependent powerstroke. Cell *147*, 209-222.

Chen, D.C., Yang, B.C., and Kuo, T.T. (1992). One-step transformation of yeast in stationary phase. Curr Genet *21*, 83-84.

Chen, H., Zhou, L., Wu, X., Li, R., Wen, J., Sha, J., and Wen, X. (2016). The PI3K/AKT pathway in the pathogenesis of prostate cancer. Front Biosci (Landmark Ed) *21*, 1084-1091.

Chi, R.J., Liu, J., West, M., Wang, J., Odorizzi, G., and Burd, C.G. (2014). Fission of SNX-BAR-coated endosomal retrograde transport carriers is promoted by the dynamin-related protein Vps1. J Cell Biol *204*, 793-806.

Chia, P.Z., Gunn, P., and Gleeson, P.A. (2013). Cargo trafficking between endosomes and the trans-Golgi network. Histochem Cell Biol *140*, 307-315.

Chiaruttini, N., Redondo-Morata, L., Colom, A., Humbert, F., Lenz, M., Scheuring, S., and Roux, A. (2015). Relaxation of Loaded ESCRT-III Spiral Springs Drives Membrane Deformation. Cell *163*, 866-879.

Cooper, A.A., and Stevens, T.H. (1996). Vps10p cycles between the late-Golgi and prevacuolar compartments in its function as the sorting receptor for multiple yeast vacuolar hydrolases. J Cell Biol *133*, 529-541.

Cowles, C.R., Snyder, W.B., Burd, C.G., and Emr, S.D. (1997). Novel Golgi to vacuole delivery pathway in yeast: identification of a sorting determinant and required transport component. EMBO J *16*, 2769-2782.

Delprato, A., and Lambright, D.G. (2007). Structural basis for Rab GTPase activation by VPS9 domain exchange factors. Nat Struct Mol Biol *14*, 406-412.

Dennes, A., Madsen, P., Nielsen, M.S., Petersen, C.M., and Pohlmann, R. (2002). The yeast Vps10p cytoplasmic tail mediates lysosomal sorting in mammalian cells and interacts with human GGAs. J Biol Chem *277*, 12288-12293.

Donaldson, J.G., and Jackson, C.L. (2011). ARF family G proteins and their regulators: roles in membrane transport, development and disease. Nat Rev Mol Cell Biol *12*, 362-375.

Dutta, D., and Donaldson, J.G. (2015). Rab and Arf G proteins in endosomal trafficking. Methods Cell Biol *130*, 127-138.

Elkin, S.R., Lakoduk, A.M., and Schmid, S.L. (2016). Endocytic pathways and endosomal trafficking: a primer. Wien Med Wochenschr.

Faelber, K., Held, M., Gao, S., Posor, Y., Haucke, V., Noe, F., and Daumke, O. (2012). Structural insights into dynamin-mediated membrane fission. Structure *20*, 1621-1628.

Furuta, N., Fujimura-Kamada, K., Saito, K., Yamamoto, T., and Tanaka, K. (2007). Endocytic recycling in yeast is regulated by putative phospholipid translocases and the Ypt31p/32p-Rcy1p pathway. Mol Biol Cell *18*, 295-312.

Gerrard, S.R., Levi, B.P., and Stevens, T.H. (2000). Pep12p is a multifunctional yeast syntaxin that controls entry of biosynthetic, endocytic and retrograde traffic into the prevacuolar compartment. Traffic *1*, 259-269.

Gill, D.J., Teo, H., Sun, J., Perisic, O., Veprintsev, D.B., Emr, S.D., and Williams, R.L. (2007). Structural insight into the ESCRT-I/-II link and its role in MVB trafficking. EMBO J *26*, 600-612.

Goddard, M.A., Mack, D.L., Czerniecki, S.M., Kelly, V.E., Snyder, J.M., Grange, R.W., Lawlor, M.W., Smith, B.K., Beggs, A.H., and Childers, M.K. (2015). Muscle pathology, limb strength, walking gait, respiratory function and neurological impairment establish disease progression in the p.N155K canine model of X-linked myotubular myopathy. Ann Transl Med *3*, 262.

Gowda, N.K., Kandasamy, G., Froehlich, M.S., Dohmen, R.J., and Andreasson, C. (2013). Hsp70 nucleotide exchange factor Fes1 is essential for ubiquitin-dependent degradation of misfolded cytosolic proteins. Proc Natl Acad Sci U S A *110*, 5975-5980.

Hayden, J., Williams, M., Granich, A., Ahn, H., Tenay, B., Lukehart, J., Highfill, C., Dobard, S., and Kim, K. (2013). Vps1 in the late endosome-to-vacuole traffic. J Biosci *38*, 73-83.

Henne, W.M., Buchkovich, N.J., and Emr, S.D. (2011). The ESCRT pathway. Dev Cell *21*, 77-91.

Henne, W.M., Stenmark, H., and Emr, S.D. (2013). Molecular mechanisms of the membrane sculpting ESCRT pathway. Cold Spring Harb Perspect Biol *5*.

Hoppins, S., Collins, S.R., Cassidy-Stone, A., Hummel, E., Devay, R.M., Lackner, L.L., Westermann, B., Schuldiner, M., Weissman, J.S., and Nunnari, J. (2011). A mitochondrial-focused genetic interaction map reveals a scaffold-like complex required for inner membrane organization in mitochondria. J Cell Biol *195*, 323-340.

Huotari, J., and Helenius, A. (2011). Endosome maturation. EMBO J *30*, 3481-3500.

Hurley, J.H., and Emr, S.D. (2006). The ESCRT complexes: structure and mechanism of a membrane-trafficking network. Annu Rev Biophys Biomol Struct *35*, 277-298.

Im, Y.J., and Hurley, J.H. (2008). Integrated structural model and membrane targeting mechanism of the human ESCRT-II complex. Dev Cell *14*, 902-913.

Janse, D.M., Crosas, B., Finley, D., and Church, G.M. (2004). Localization to the proteasome is sufficient for degradation. J Biol Chem *279*, 21415-21420.

Jonikas, M.C., Collins, S.R., Denic, V., Oh, E., Quan, E.M., Schmid, V., Weibezahn, J., Schwappach, B., Walter, P., Weissman, J.S.*, et al.* (2009). Comprehensive characterization of genes required for protein folding in the endoplasmic reticulum. Science *323*, 1693-1697.

Kim, S., Sato, Y., Mohan, P.S., Peterhoff, C., Pensalfini, A., Rigoglioso, A., Jiang, Y., and Nixon, R.A. (2016). Evidence that the rab5 effector APPL1 mediates APP-betaCTF-induced dysfunction of endosomes in Down syndrome and Alzheimer's disease. Mol Psychiatry *21*, 707-716.

Kostelansky, M.S., Schluter, C., Tam, Y.Y., Lee, S., Ghirlando, R., Beach, B., Conibear, E., and Hurley, J.H. (2007). Molecular architecture and functional model of the complete yeast ESCRT-I heterotetramer. Cell *129*, 485-498.

Kostelansky, M.S., Sun, J., Lee, S., Kim, J., Ghirlando, R., Hierro, A., Emr, S.D., and Hurley, J.H. (2006). Structural and functional organization of the ESCRT-I trafficking complex. Cell *125*, 113-126.

Kulkarni, A., Alpadi, K., Sirupangi, T., and Peters, C. (2014a). A dynamin homolog promotes the transition from hemifusion to content mixing in intracellular membrane fusion. Traffic (Copenhagen, Denmark).

Kulkarni, A., Alpadi, K., Sirupangi, T., and Peters, C. (2014b). A dynamin homolog promotes the transition from hemifusion to content mixing in intracellular membrane fusion. Traffic *15*, 558-571.

Kuravi, K., Nagotu, S., Krikken, A.M., Sjollema, K., Deckers, M., Erdmann, R., Veenhuis, M., and van der Klei, I.J. (2006). Dynamin-related proteins Vps1p and Dnm1p control peroxisome abundance in Saccharomyces cerevisiae. J Cell Sci *119*, 3994-4001.

Lawlor, M.W., Beggs, A.H., Buj-Bello, A., Childers, M.K., Dowling, J.J., James, E.S., Meng, H., Moore, S.A., Prasad, S., Schoser, B.*, et al.* (2016). Skeletal Muscle Pathology in X-Linked Myotubular Myopathy: Review With Cross-Species Comparisons. J Neuropathol Exp Neurol.

Lilienbaum, A. (2013). Relationship between the proteasomal system and autophagy. Int J Biochem Mol Biol *4*, 1-26.

Lin, P., Liu, X., Zhao, D., Dai, T., Wu, H., Gong, Y., and Yan, C. (2016). DNM2 mutations in Chinese Han patients with centronuclear myopathy. Neurol Sci.

Lippe, R., Miaczynska, M., Rybin, V., Runge, A., and Zerial, M. (2001). Functional synergy between Rab5 effector Rabaptin-5 and exchange factor Rabex-5 when physically associated in a complex. Mol Biol Cell *12*, 2219-2228.

Liu, K., Jian, Y., Sun, X., Yang, C., Gao, Z., Zhang, Z., Liu, X., Li, Y., Xu, J., Jing, Y.*, et al.* (2016). Negative regulation of phosphatidylinositol 3-phosphate levels in early-to-late endosome conversion. J Cell Biol *212*, 181-198.

Liu, Y.W., Lukiyanchuk, V., and Schmid, S.L. (2011). Common membrane trafficking defects of disease-associated dynamin 2 mutations. Traffic *12*, 1620-1633.

Lukehart, J., Highfill, C., and Kim, K. (2013). Vps1, a recycling factor for the traffic from early endosome to the late Golgi. Biochem Cell Biol *91*, 455-465.

MacDonald, E., Urbe, S., and Clague, M.J. (2014). USP8 controls the trafficking and sorting of lysosomal enzymes. Traffic *15*, 879-888.

Mageswaran, S.K., Johnson, N.K., Odorizzi, G., and Babst, M. (2015). Constitutively active ESCRT-II suppresses the MVB-sorting phenotype of ESCRT-0 and ESCRT-I mutants. Mol Biol Cell *26*, 554-568.

Marat, A.L., and Haucke, V. (2016). Phosphatidylinositol 3-phosphates-at the interface between cell signalling and membrane traffic. EMBO J *35*, 561-579.

Mears, J.A., Lackner, L.L., Fang, S., Ingerman, E., Nunnari, J., and Hinshaw, J.E. (2011). Conformational changes in Dnm1 support a contractile mechanism for mitochondrial fission. Nat Struct Mol Biol *18*, 20-26.

Mehrotra, N., Nichols, J., and Ramachandran, R. (2014). Alternate pleckstrin homology domain orientations regulate dynamin-catalyzed membrane fission. Mol Biol Cell *25*, 879-890.

Meissner, D., Odman-Naresh, J., Vogelpohl, I., and Merzendorfer, H. (2010). A novel role of the yeast CaaX protease Ste24 in chitin synthesis. Mol Biol Cell *21*, 2425-2433.

Meng, B., Ip, N.C., Prestwood, L.J., Abbink, T.E., and Lever, A.M. (2015). Evidence that the endosomal sorting complex required for transport-II (ESCRT-II) is required for efficient human immunodeficiency virus-1 (HIV-1) production. Retrovirology *12*, 72.

Munsie, L.N., Milnerwood, A.J., Seibler, P., Beccano-Kelly, D.A., Tatarnikov, I., Khinda, J., Volta, M., Kadgien, C., Cao, L.P., Tapia, L.*, et al.* (2015). Retromer-dependent neurotransmitter receptor trafficking to synapses is altered by the Parkinson's disease VPS35 mutation p.D620N. Hum Mol Genet *24*, 1691-1703.

Neel, B.A., Zong, H., Backer, J.M., and Pessin, J.E. (2015). Identification of Atypical Peri-Nuclear Multivesicular Bodies in Oxidative and Glycolytic Skeletal Muscle of Aged and Pompe's Disease Mouse Models. Front Physiol *6*, 393.

Nickerson, D.P., Russell, M.R., and Odorizzi, G. (2007). A concentric circle model of multivesicular body cargo sorting. EMBO Rep *8*, 644-650.

Nickerson, D.P., West, M., Henry, R., and Odorizzi, G. (2010). Regulators of Vps4 ATPase activity at endosomes differentially influence the size and rate of formation of intralumenal vesicles. Mol Biol Cell *21*, 1023-1032.

Nielsen, E., Christoforidis, S., Uttenweiler-Joseph, S., Miaczynska, M., Dewitte, F., Wilm, M., Hoflack, B., and Zerial, M. (2000). Rabenosyn-5, a novel Rab5 effector, is complexed with hVPS45 and recruited to endosomes through a FYVE finger domain. J Cell Biol *151*, 601-612.

Noma, S., Iida, K., and Iida, H. (2005). Polarized morphogenesis regulator Spa2 is required for the function of putative stretch-activated Ca2+-permeable channel component Mid1 in Saccharomyces cerevisiae. Eukaryot Cell *4*, 1353-1363.

Nothwehr, S.F., Conibear, E., and Stevens, T.H. (1995). Golgi and vacuolar membrane proteins reach the vacuole in vps1 mutant yeast cells via the plasma membrane. J Cell Biol *129*, 35-46.

Obara, K., Kojima, R., and Kihara, A. (2013). Effects on vesicular transport pathways at the late endosome in cells with limited very long-chain fatty acids. J Lipid Res *54*, 831-842.

Odorizzi, G., Katzmann, D.J., Babst, M., Audhya, A., and Emr, S.D. (2003). Bro1 is an endosome-associated protein that functions in the MVB pathway in Saccharomyces cerevisiae. J Cell Sci *116*, 1893-1903.

Palmer, S.E., Smaczynska-de, R., II, Marklew, C.J., Allwood, E.G., Mishra, R., Goldberg, M.W., and Ayscough, K.R. (2015). A Charge Swap mutation E461K in the yeast dynamin Vps1 reduces endocytic invagination. Commun Integr Biol *8*, e1051274.

Poteryaev, D., Datta, S., Ackema, K., Zerial, M., and Spang, A. (2010). Identification of the switch in early-to-late endosome transition. Cell *141*, 497-508.

Pryor, E.E., Jr., Horanyi, P.S., Clark, K.M., Fedoriw, N., Connelly, S.M., Koszelak-Rosenblum, M., Zhu, G., Malkowski, M.G., Wiener, M.C., and Dumont, M.E. (2013). Structure of the integral membrane protein CAAX protease Ste24p. Science *339*, 1600-1604.

Raiborg, C., Bremnes, B., Mehlum, A., Gillooly, D.J., D'Arrigo, A., Stang, E., and Stenmark, H. (2001). FYVE and coiled-coil domains determine the specific localisation of Hrs to early endosomes. J Cell Sci *114*, 2255-2263.

Ren, X., and Hurley, J.H. (2010). VHS domains of ESCRT-0 cooperate in high-avidity binding to polyubiquitinated cargo. EMBO J *29*, 1045-1054.

Robinson, F.L., and Dixon, J.E. (2006). Myotubularin phosphatases: policing 3-phosphoinositides. Trends Cell Biol *16*, 403-412.

Robinson, J.S., Klionsky, D.J., Banta, L.M., and Emr, S.D. (1988). Protein sorting in Saccharomyces cerevisiae: isolation of mutants defective in the delivery and processing of multiple vacuolar hydrolases. Mol Cell Biol *8*, 4936-4948.

Sestak, S., Hagen, I., Tanner, W., and Strahl, S. (2004). Scw10p, a cell-wall glucanase/transglucosidase important for cell-wall stability in Saccharomyces cerevisiae. Microbiology *150*, 3197-3208.

Shenoy, S.K. (2007). Seven-transmembrane receptors and ubiquitination. Circ Res *100*, 1142-1154.

Sheu, Y.J., Santos, B., Fortin, N., Costigan, C., and Snyder, M. (1998). Spa2p interacts with cell polarity proteins and signaling components involved in yeast cell morphogenesis. Mol Cell Biol *18*, 4053-4069.

Shields, S.B., Oestreich, A.J., Winistorfer, S., Nguyen, D., Payne, J.A., Katzmann, D.J., and Piper, R. (2009). ESCRT ubiquitin-binding domains function cooperatively during MVB cargo sorting. J Cell Biol *185*, 213-224.

Silva, P., Mendoza, P., Rivas, S., Diaz, J., Moraga, C., Quest, A.F., and Torres, V.A. (2016). Hypoxia promotes Rab5 activation, leading to tumor cell migration, invasion and metastasis. Oncotarget.

Sirisaengtaksin, N., Gireud, M., Yan, Q., Kubota, Y., Meza, D., Waymire, J.C., Zage, P.E., and Bean, A.J. (2014). UBE4B protein couples ubiquitination and sorting machineries to enable epidermal growth factor receptor (EGFR) degradation. J Biol Chem *289*, 3026-3039.

Smaczynska-de, R., II, Allwood, E.G., Aghamohammadzadeh, S., Hettema, E.H., Goldberg, M.W., and Ayscough, K.R. (2010). A role for the dynamin-like protein Vps1 during endocytosis in yeast. Journal of cell science *123*, 3496-3506.

Smaczynska-de, R., II, Marklew, C.J., Allwood, E.G., Palmer, S.E., Booth, W.I., Mishra, R., Goldberg, M.W., and Ayscough, K.R. (2015). Phosphorylation Regulates the Endocytic Function of the Yeast Dynamin-Related Protein Vps1. Mol Cell Biol *36*, 742-755.

Smaczynska-de Rooij, I.I., Allwood, E.G., Aghamohammadzadeh, S., Hettema, E.H., Goldberg, M.W., and Ayscough, K.R. (2010). A role for the dynamin-like protein Vps1 during endocytosis in yeast. J Cell Sci *123*, 3496-3506.

Snyder, M. (1989). The SPA2 protein of yeast localizes to sites of cell growth. J Cell Biol *108*, 1419-1429.

Starr, T.L., Pagant, S., Wang, C.W., and Schekman, R. (2012). Sorting signals that mediate traffic of chitin synthase III between the TGN/endosomes and to the plasma membrane in yeast. PLoS One *7*, e46386.

Stenmark, H. (2009). Rab GTPases as coordinators of vesicle traffic. Nat Rev Mol Cell Biol *10*, 513-525.

Sundborger, A.C., and Hinshaw, J.E. (2014). Regulating dynamin dynamics during endocytosis. F1000Prime Rep *6*, 85.

Surma, M.A., Klose, C., Peng, D., Shales, M., Mrejen, C., Stefanko, A., Braberg, H., Gordon, D.E., Vorkel, D., Ejsing, C.S.*, et al.* (2013). A lipid E-MAP identifies Ubx2 as a critical regulator of lipid saturation and lipid bilayer stress. Mol Cell *51*, 519-530.

Takahashi, H., Mayers, J.R., Wang, L., Edwardson, J.M., and Audhya, A. (2015). Hrs and STAM function synergistically to bind ubiquitin-modified cargoes in vitro. Biophys J *108*, 76-84.

Tang, S., Buchkovich, N.J., Henne, W.M., Banjade, S., Kim, Y.J., and Emr, S.D. (2016). ESCRT-III activation by parallel action of ESCRT-I/II and ESCRT-0/Bro1 during MVB biogenesis. Elife *5*.

Teis, D., Saksena, S., Judson, B.L., and Emr, S.D. (2010). ESCRT-II coordinates the assembly of ESCRT-III filaments for cargo sorting and multivesicular body vesicle formation. EMBO J *29*, 871-883.

Teo, H., Perisic, O., González, B., and Williams, R.L. (2004a). ESCRT-II, an endosome-associated complex required for protein sorting: crystal structure and interactions with ESCRT-III and membranes. Dev Cell *7*, 559-569.

Teo, H., Veprintsev, D.B., and Williams, R.L. (2004b). Structural insights into endosomal sorting complex required for transport (ESCRT-I) recognition of ubiquitinated proteins. J Biol Chem *279*, 28689-28696.

Thorn, P., Zorec, R., Rettig, J., and Keating, D.J. (2016). Exocytosis in non-neuronal cells. J Neurochem.

Urbe, S. (2005). Ubiquitin and endocytic protein sorting. Essays Biochem *41*, 81-98.

Virag, A., and Harris, S.D. (2006). Functional characterization of Aspergillus nidulans homologues of Saccharomyces cerevisiae Spa2 and Bud6. Eukaryot Cell *5*, 881-895.

Wang, G., and Wu, G. (2012). Small GTPase regulation of GPCR anterograde trafficking. Trends Pharmacol Sci *33*, 28-34.

Williams, M., and Kim, K. (2014). From membranes to organelles: Emerging roles for dynamin-like proteins in diverse cellular processes. Eur J Cell Biol *93*, 267-277.

Wollert, T., and Hurley, J.H. (2010). Molecular mechanism of multivesicular body biogenesis by ESCRT complexes. Nature *464*, 864-869.

Wollert, T., Wunder, C., Lippincott-Schwartz, J., and Hurley, J.H. (2009). Membrane scission by the ESCRT-III complex. Nature *458*, 172-177.

Woodman, P. (2016). ESCRT-III on endosomes: new functions, new activation pathway. The Biochemical journal *473*, e5-8.

Yasuda, S., Morishita, S., Fujita, A., Nanao, T., Wada, N., Waguri, S., Schiavo, G., Fukuda, M., and Nakamura, T. (2016). Mon1-Ccz1 activates Rab7 only on late endosomes and dissociates from the lysosome in mammalian cells. J Cell Sci *129*, 329-340.

Yu, X., and Cai, M. (2004). The yeast dynamin-related GTPase Vps1p functions in the organization of the actin cytoskeleton via interaction with Sla1p. J Cell Sci *117*, 3839-3853.

Zarrinpar, A., Bhattacharyya, R.P., Nittler, M.P., and Lim, W.A. (2004). Sho1 and Pbs2 act as coscaffolds linking components in the yeast high osmolarity MAP kinase pathway. Mol Cell *14*, 825-832.

Zeigerer, A., Gilleron, J., Bogorad, R.L., Marsico, G., Nonaka, H., Seifert, S., Epstein-Barash, H., Kuchimanchi, S., Peng, C.G., Ruda, V.M.*, et al.* (2012). Rab5 is necessary for the biogenesis of the endolysosomal system in vivo. Nature *485*, 465-470.

Zhu, H., Qian, H., and Li, G. (2010). Delayed onset of positive feedback activation of Rab5 by Rabex-5 and Rabaptin-5 in endocytosis. PLoS One *5*, e9226.

Zolov, S.N., Bridges, D., Zhang, Y., Lee, W.W., Riehle, E., Verma, R., Lenk, G.M., Converso-Baran, K., Weide, T., Albin, R.L.*, et al.* (2012). In vivo, Pikfyve generates PI(3,5)P2, which serves as both a signaling lipid and the major precursor for PI5P. Proc Natl Acad Sci U S A *109*, 17472-17477.